

# The Southern Flanking Fields of the 25 Orionis Group

Peregrine M. McGehee<sup>1</sup>

## ABSTRACT

The stellar group surrounding the Be (B1Vpe) star 25 Orionis was discovered to be a pre-main-sequence population by the Centro de Investigaciones de Astronomia (CIDA) Orion Variability Survey and subsequent spectroscopy. We analyze Sloan Digital Sky Survey multi-epoch photometry to map the southern extent of the 25 Ori group and to characterize its pre-main-sequence population. We compare this group to the neighboring Orion OB1a and OB1b subassociations and to active star formation sites (NGC 2068/NGC 2071) within the Lynds 1630 dark cloud. We find that the 25 Ori group has a radius of  $1.4^\circ$ , corresponding to 8-11 pc at the distances of Orion OB1a and OB1b. Given that the characteristic sizes of young open clusters are a few pc or less this suggests that 25 Ori is an unbound association rather than an open cluster. Due to its PMS population having a low Classical T Tauri fraction ( $\sim 10\%$ ) we conclude that the 25 Ori group is of comparable age to the 11 Myr Orion OB1a subassociation.

*Subject headings:* open clusters and associations: individual (25 Orionis) – stars: formation – stars: late-type – stars: low-mass, brown dwarfs – stars: pre-main-sequence

## 1. Introduction

The pre-main-sequence 25 Orionis group has been recently identified by the Centro de Investigaciones de Astronomia Variability Survey of Orion (CVSO; Briceño et al. 2005a) on the basis of multi-epoch imaging and follow-up spectroscopy. 25 Ori has also been noted by Kharchenko et al. (2005) as a candidate open cluster, ASCC 16, based on analysis of the All-Sky Compiled Catalogue of 2.5 Million Stars (ASCC-2.5; Kharchenko 2001). This group is named after the Be star 25 Orionis,  $(\alpha_{2000}, \delta_{2000}) = (05^h 24^m 44.92^s, +01^\circ 50^m 47.2^s)$  or  $(l, b) = (200.96, -18.2)$ . Spectroscopically confirmed candidate group members are found within one degree from 25 Orionis (Briceño et al. 2005b).

---

<sup>1</sup> Los Alamos National Laboratory, LANSCE-IC, MS H820, Los Alamos, NM 87545;  
peregrine@lanl.gov

We use multi-epoch imaging by the Sloan Digital Sky Survey (SDSS) to select candidate pre-main-sequence (PMS) objects based on variability and location in color-magnitude diagrams. The SDSS imaging within the Orion region spans the declination range of  $-1.25^\circ$  to  $+1.25^\circ$ , thereby covering the southern edge of the 25 Ori group within  $0.6^\circ$  of the central Be star.

In this paper we examine the PMS populations near 25 Orionis to determine the observational characteristics and spatial extent of this group. In §2 we describe the SDSS equatorial imaging survey in the Orion region. §3 revisits the classification scheme of McGehee et al. (2005) for PMS candidates based on multi-band variability. In §4 we present our results, and in §5 we discuss our findings, conclusions, and future work.

## 2. Observations

### 2.1. Photometry

The SDSS low Galactic latitude data which includes the Orion equatorial imaging used in this work are presented by Finkbeiner et al. (2004). The SDSS multi-epoch imaging data used in this paper as well as the selection for candidate low-mass pre-main sequence objects are discussed in McGehee et al. (2005). Here we describe the salient features of the SDSS drift-scanned imaging.

The SDSS obtains deep photometry with asinh magnitude (Lupton, Gunn, & Szalay 1999) limits (defined by 95% detection repeatability for point sources) of  $u = 22.0$ ,  $g = 22.2$ ,  $r = 22.2$ ,  $i = 21.2$  and  $z = 20.5$ . These five passbands,  $ugriz$ , have effective wavelengths of 3540, 4760, 6290, 7690, and 9250 Å, respectively. A technical summary of the SDSS is given by York et al. (2000). The SDSS imaging camera and telescope are described by Gunn et al. (1998) and Gunn et al. (2006), respectively. Ivezić et al. (2004) discuss the data management and photometric quality assessment system.

The Early Data Release and the Data Release One are described by Stoughton et al. (2002) and Abazajian et al. (2003). The former includes an extensive discussion of the data outputs and software. Pier et al. (2003) describe the astrometric calibration of the survey and the network of primary photometric standard stars is described by Smith et al. (2002). The photometric system itself is defined by Fukugita et al. (1996), and the system which monitors the site photometricity by Hogg et al. (2001). Abazajian et al. (2003) discuss the differences between the native SDSS 2.5m  $ugriz$  system and the  $u'g'r'i'z'$  standard star system defined on the USNO 1.0 m (Smith et al. 2002). The Two-Micron All Sky Survey 2MASS (2MASS; Skrutskie et al. 1997) obtained nearly complete coverage of the sky in

$JHK_s$ .

## 2.2. Comparison of CIDA and SDSS Survey Coverage

The SDSS Orion equatorial data consist of a  $2.5^\circ$  wide stripe centered on the celestial equator. For this work we consider the  $37.5 \text{ deg}^2$  bounded in R.A. by  $5^h$  to  $6^h$  that lies completely within the CVSO survey region. While the temporal sampling by the SDSS imaging is much sparser with at most 7 observations per target over a span of nearly 5 years, the SDSS survey is deeper and thus is able to detect low-mass and very-low-mass objects.

There are 197 spectroscopically confirmed Weak-lined T Tauris (WTTS) and Classical T Tauris (CTTS) found by the CVSO survey (Briceño et al. 2005a). Out of the 76 that are located within the SDSS equatorial scans, we find that 10 are identified in the SDSS low-mass star study (McGehee et al. 2005) which selected for M dwarf colored stars on the basis of  $(r - i) > 0.6$  and  $Q_{riz} > 0.35$ , where the latter is a reddening-invariant index formed by the SDSS  $riz$  magnitudes (see §3.1 below). These matches are listed in Table 1. The complete set of WTTS and CTTS candidates identified in the SDSS survey are presented in Table 2. These tables include object classification based on multi-band variability into non-PMS, WTTS, and CTTS as discussed in §3.2 below. Within §3.3 we investigate the effectiveness of selection and classification of PMS objects based solely on variability.

The objects detected by the SDSS low-mass star survey are both faint ( $V > 15.7$ ) and red ( $V - I_C > 2.2$ ), as evident in Figure 1. The single faint object that was not selected by McGehee et al. (2005) is CVSO 157, a highly veiled continuum CTTS, whose  $r - i$  and  $Q_{riz}$  colors were in the ranges 0.42 to 0.77 and -0.50 to -0.11, respectively.

## 3. Identification of CTTS Candidates

### 3.1. Reddening-Invariant Indices

The Orion OB1a and OB1b subassociations comprise a range of star formation environments ranging from older, dispersed populations having low line-of-sight interstellar extinction to very young and embedded systems, such as those associated with the Lynds 1630 dark cloud (Lynds 1962). In order to mitigate the need to deredden the photometry for each object we utilize a number of reddening-invariant indices (colors) and magnitudes to aid in the classification of the stars in these regions

In this work we employ reddening-invariant indices of the form  $Q_{xyz} = (x - y) - (y - z) \times$

$E(x - y)/E(y - z)$ . For passbands defined at wavelengths less than  $1\mu\text{m}$ ,  $Q_{xyz}$  is dependent upon the assumed ratio of general to selective extinction ( $R_V = A_V/E(B - V)$ ; Cardelli, Clayton, & Mathis (1989)). Here  $xyz$  refer to the specific passbands, e.g.  $ugrizJHK_S$ , and  $E(x - y)$  is the color excess due to reddening of the  $x - y$  color. This definition of reddening-invariant colors follows Johnson & Morgan (1953) in that in our notation their original  $Q$  would be written as  $Q_{UBV}$ . In the  $(x - y, y - z)$  color-color diagram the  $Q_{xyz}$  axis is perpendicular to the reddening vector. These indices are discussed in full by McGehee et al. (2005).

We use the extinction tables derived by D. Finkbeiner<sup>1</sup> to define the coefficients used in defining reddening-invariant colors. These tables contain the  $A_X/E(B - V)$  values for the SDSS  $ugriz$  filters for specific values of  $R_V$  and source spectra. The values we present here are obtained using an F dwarf source spectrum and  $R_V = 3.1$  which is the standard extinction law found in the diffuse ISM.

In this work we use optical and near-IR indices  $Q_{riz} = (r - i) - 0.987(i - z)$  and  $Q_{JHK} = (J - H) - 1.563(H - K)$ . We also employ reddening-invariant magnitudes constructed from linear combinations of observed magnitudes and colors. Here we use a near-IR reddening-invariant magnitude  $J_{J-H} = J - (J - H)A_J/E(J - H) = J - 2.76(J - H)$ . The numerical terms in the  $Q_{JHK}$  and  $J_{J-H}$  definitions are based on the reddening coefficients of Schlegel, Finkbeiner, & Davis (1998). The notation follows that of Babusiaux & Gilmore (2005) who used  $K_{sJ-K_s}$  to determine distances to red clump stars in the inner Galactic bulge. We chose the combination of the  $J$  and  $H$  bands to minimize the effect of thermal emission from the inner circumstellar disk.

### 3.2. Comparison of Variability and Near-IR Disk Indicators

In McGehee et al. (2005) we identified candidate PMS objects on the basis of  $\sigma_g > 0.05$ , where the subset flagged as possible CTTS rather than WTTS were selected by  $\sigma_z > 0.05$ . Here  $\sigma_g$  and  $\sigma_z$  are the standard deviations in the  $g$  and  $z$  bands measured over all observations for a star. Application of these criteria to a comparison field yielded possible contamination fractions of 8.7% for all PMS candidates (WTTS and CTTS) and of 2.9% for CTTS only. The majority of the contaminants are likely foreground active M dwarfs (dMe).

In this work we improve these selection criteria by comparing the SDSS multi-band variability against the intrinsic near-IR excess computed from 2MASS observations. This

---

<sup>1</sup>private communication; see <http://www.astro.princeton.edu/~dfink/sdssfilters/>

procedure assumes that the high-amplitude variability and near-IR excess are both due to the presence of an inner circumstellar disk with the former generated by magnetosospheric accretion processes and the latter by disk thermal emission.

Due to the low-mass and very-low-mass nature of our sample we need to be concerned about the contrast between the stellar photospheric emission and that from the inner circumstellar disk. Liu, Najita, & Tokunaga (2003) note that the  $K$  band excess vanishes for spectral types of M6 and later, thereby making use of longer wavelength bands such as  $L$  and  $M$  critical for detection of circumstellar disks around very-low-mass stars and young brown dwarfs. In Figure 2 we see that, based on the Baraffe et al. (1998) [BCAH98] isochrones and the Luhman (2003) PMS temperature scale, a 2 Myr old star in the Orion OB1b subassociation with a spectral type between M5 and M6 would have  $J_{J-H} = 12.0$ . We adopt this as the faint magnitude limit for reliable detection of  $K$  band disk emission in our study.

We begin by defining a reddening-invariant near-IR excess,  $\Delta Q_{JHK}$ , relative to the stellar locus in the  $(Q_{JHK}, J_{J-H})$  color-magnitude diagram. In Figure 3 we present the BCAH98 isochrones for Orion OB1a and Orion OB1b in this reddening-invariant near-IR color-magnitude diagram. The steepening of the stellar locus for the brighter stars motivates us to define a bright limit of  $J_{J-H} = 9.6$ . The isochrones for Orion OB1a and OB1b lie nearly on top of each other for  $9.6 < J_{J-H} < 12.0$ . A least-squares fit gives  $Q_{JHK} = 1.986 - 0.157J_{J-H}$  in this magnitude range, thus we define  $\Delta Q_{JHK} = Q_{JHK} - (1.986 - 0.157J_{J-H})$ .

In order to determine the reddening-invariant colors of disk candidates we first consider the CTTS locus of Meyer, Calvet, & Hillenbrand (1997) which, in the  $(J-H, H-K)$  color-color diagram, is  $(J-H) = 0.58(H-K) + 0.52$ . For a star on the CTTS locus an increase in  $(H-K)$  of  $\delta(H-K)$  implies  $\delta Q_{JHK} = -0.98\delta(H-K)$  and  $\delta J_{J-H} = 0.58\delta(H-K)$  with the resulting  $\delta \Delta Q_{JHK} = -1.23\delta(H-K)$ . Therefore we expect CTTS candidates to have  $\Delta Q_{JHK} < 0$ , that is, found to the left of the stellar locus in the  $(Q_{JHK}, J_{J-H})$  diagram.

Examination of Figures 4 and 5, in which the standard deviations in  $g$  and  $z$  are compared against  $\Delta Q_{JHK}$  for stars having  $9.6 < J_{J-H} < 12.0$ , reveals that the criteria used by McGehee et al. (2005) for detection of CTTS candidates are insufficiently stringent. Specifically, the threshold for variability in the  $g$  band that matches the onset of significant near-IR excess is  $\sigma_g = 0.2$ , i.e., a factor of four greater than used in McGehee et al. (2005). The stars selected by these new criteria (*diamonds*) and having  $J_{J-H} < 12$  show near-IR excess in the  $(Q_{JHK}, J_{J-H})$  CMD (Figure 3).

### 3.3. The Effectiveness of Classification by Variability Alone

We see in Table 1 that some discrepancies exist between the results of the variability-based classification scheme in this work and those obtained by analysis of optical spectra in Briceño et al. (2005b). Out of the 7 WTTS we find that the SDSS survey agrees on 4 objects, classing the remaining 3 as non-PMS. For the 3 confirmed CTTS, we class 2 as WTTS and 1 as non-PMS.

We use the full sample of Briceño et al. (2005b) to assess the effectiveness of distinguishing WTTS and CTTS based on a threshold value of  $\sigma_V$ . For each threshold value of  $\sigma_V$  we identify WTTS candidates as those with  $\sigma_V$  below this threshold and CTTS candidates those RMS values exceed this threshold. In this collection of stars from both the Orion OB1a and OB1b subassociations there are  $N_{WTTS} = 138$  WTTS and  $N_{CTTS} = 38$  CTTS, giving a CTTS or inner disk fraction of 21.7%. We begin by examining the Cumulative Distribution Function (CDF) for  $\sigma_V$  for both types of PMS stars. In Figure 6 we see that while the CTTS clearly tend to have higher  $\sigma_V$  values than the WTTS, there do exist both high-amplitude WTTS and low-amplitude CTTS, thus using the amplitude or, in our case, the RMS of the variability will not be perfectly efficient.

To measure the selection efficiency we consider two selection metrics, the accuracy and the computed CTTS fraction. In order to assess the ability to classify individual stars as WTTS or CTTS we use the accuracy, defined as

$$Accuracy = \frac{N_{TP}}{N_{CTTS}} - \frac{N_{FP}}{N_{WTTS}} \quad (1)$$

where  $N_{TP}$  and  $N_{FP}$  are the number of true positives and false positives, respectively. We also look at computed CTTS fraction, given by

$$f_{CTTS} = \frac{N_{TP} + N_{FP}}{N_{CTTS} + N_{WTTS}}. \quad (2)$$

In Figure 7 we plot both of these selection metrics against the threshold value of  $\sigma_V$ . We find that the peak accuracy of  $\sim 0.4$  is found for a threshold value of 0.1 magnitudes and that the computed CTTS fraction is close to the actual CTTS fraction for  $\sigma_V$  thresholds between 0.1 and 0.15 magnitudes. Since the variability amplitude in CTTS increases sharply at shorter wavelengths, with typical values of  $\sigma_B/\sigma_V \sim 1.3$  (Herbst et al. 1994), we might expect that the optimal threshold for WTTS/CTTS differentiation using the SDSS  $g$  band, which has a similar effective wavelength as  $B$ , may be in the range of 0.13 to 0.2 magnitudes. This suggests that the computed CTTS fraction in our work, which is based on a  $\sigma_g$  threshold of 0.2 magnitudes, may not be unreasonable.

## 4. Results

### 4.1. Distribution

The 25 Orionis group is evident in a surface density plot of candidate PMS stars that are identified on the basis of  $\sigma_g > 0.05$ . In Figure 8 there are three obvious groupings of PMS stars which, in order of increasing R.A., are the 25 Ori group, the Orion OB1b subassociation, and the NGC 2068/NGC 2071 star formation site in the L1630 cloud. The surface densities are computed on a  $1.0^\circ$  by  $0.25^\circ$  grid in R.A. and Dec. with the peak value of 68 stars  $\text{deg}^{-2}$  found at the center of the Ori OB1b subassociation.

We look for the southern extent of the 25 Ori group by computing the surface density of the PMS candidates as a function of radial distance from the Be star 25 Orionis. Due to the center of the group being outside of the SDSS imaging area we compute the areas for each radial bin as  $\int_r^{r+\Delta r} 2r\cos^{-1}(d/r)dr$  where the radial bin size  $\Delta r = 0.4^\circ$ , the distance between 25 Ori and the SDSS imaging area  $d = 0.6^\circ$ , and  $r \geq d$ .

In Figure 9 we see that the 25 Ori group blends into the surrounding dispersed PMS population of Ori OB1a at distances greater than  $1.4^\circ$  from the Be star 25 Orionis. In contrast, the NGC 2068/NGC 2071 complex is much more compact and contained within a radius of  $0.6^\circ$ , as measured from the center of NGC 2071. The near-IR survey of (Lada et al. 1991) of L1630, complete to  $K = 13$ , showed that the four active star formation sites in L1630 are tightly clustered with typical effective radii of  $0.1^\circ$  or less. Therefore most of this spatial extent is accounted for by the  $0.3^\circ$  separation between individual NGC 2068 and NGC 2071 protoclusters. Furthermore, the submillimeter dust continuum study of NGC 2068/NGC 2071 at  $450 \mu\text{m}$  and  $850 \mu\text{m}$  by Motte et al. (2001) shows that each of these protoclusters consist of filamentary dense cores.

In Figure 10, which plots the individual stars within a  $4^\circ$  by  $4^\circ$  region centered on 25 Orionis, the clustering of candidate PMS objects around the central Be star is evident. For comparison, Figure 11 shows the same sized region around the NGC 2068/NGC 2071 star formation site. In each of these figures we identify the SDSS low-mass WTTS and CTTS candidates and the spectroscopically confirmed T Tauris from the CVSO.

### 4.2. CTTS Fraction

We examine the relative fraction of CTTS candidates, defined as  $N(\text{CTTS})/(N(\text{CTTS}) + N(\text{WTTS}))$ , using the same  $1.0^\circ$  by  $0.25^\circ$  spatial grid as used by the surface density map (Figure 8). We compute this fraction for each spatial bin that contains five or more PMS

candidates. As seen in Figure 12 the peak fraction is found in the NGC 2068/NGC 2071 complex, which is an active star formation site. The CTTS fraction is somewhat less in the  $\sim 2$  Myr Ori OB1b association, and diminished in the 25 Orionis group.

Examination of the CTTS fraction, using the radial bins defined in Figure 9, shows that the core of the L1630 site has a CTTS fraction of  $0.7 \pm 0.35$ . This is consistent with the disk fraction of  $0.85 \pm 0.15$  found by Haisch et al. (2001) for another L1630 star formation site, the 0.3 Myr NGC 2024 protocluster. In the southern flanking fields of 25 Ori, however, the CTTS fraction is  $\sim 0.1$ . This is suggestive of an relatively older population than in L1630 or Orion OB1b since the CTTS fraction decreases with age, due to typical circumstellar disk lifetimes of order 1 to 10 Myr (Kenyon & Hartmann 1995).

## 5. Discussion and Conclusions

We have mapped the southern extent of the 25 Ori group using multi-epoch imaging by the Sloan Digital Sky Survey. By studying the surface densities of PMS candidates in radial bins centered on the Be star 25 Ori, we see that the low-mass population of the 25 Ori group extends out to  $\sim 1.4^\circ$ . This corresponds to a physical radius of 8 to 11 pc, based on distances of 330 pc (for Ori OB1a) and 440 pc (for OB1b), respectively.

The majority of young ( $< 15$  Myr) clusters have radii less than a few pc (van den Bergh 2005). While there exist young clusters that have significantly larger physical dimensions these are probably not gravitationally bound. The large spatial extent of the 25 Ori group suggests that it is an unbound association, rather than a open cluster, although this is a preliminary classification based only on the southern flanking fields.

Comparison of variability and near-IR excess have led to the adoption of selection criteria for CTTS candidates based on multi-band variability that are  $\sigma_g > 0.2$  and  $\sigma_z > 0.05$ , with the  $g$  band criterion a factor of four times more restrictive than used in McGehee et al. (2005). By classifying objects on the basis of multi-band variability as probable WTTS or CTTS candidates we detect the known star formation complexes in the Orion equatorial region (L1630 and Orion OB1b) by virtue of their high CTTS fraction, with the core of the NGC 2068/NGC 2071 complex in the northern portion of the L1630 cloud having a CTTS fraction  $\sim 0.7$ .

We find that both the 25 Ori group and the Orion OB1a subassociation have CTTS fractions of  $\sim 0.1$ , similar to that found by Briceño et al. (2005b). In Figure 12. of Briceño et al. (2005b) we that this CTTS, or inner disk, fraction, is consistent with ages between 5 Myr and 30 Myr.

Future work involving this group includes mapping of the central region and detailed comparison of its structure with a number of young clusters and associations. Our goal is to determine if a gravitationally bound core to the 25 Ori group exists that may evolve into an open cluster.

We thank the anonymous referee for comments that have improved this paper. P.M.M. acknowledges support from LANL Laboratory Directed Research and Development (LDRD) program 20060495ER. Funding for the SDSS and SDSS-II has been provided by the Alfred P. Sloan Foundation, the Participating Institutions, the National Science Foundation, the U.S. Department of Energy, the National Aeronautics and Space Administration, the Japanese Monbukagakusho, the Max Planck Society, and the Higher Education Funding Council for England. The SDSS Web Site is <http://www.sdss.org/>.

The SDSS is managed by the Astrophysical Research Consortium for the Participating Institutions. The Participating Institutions are the American Museum of Natural History, Astrophysical Institute Potsdam, University of Basel, Cambridge University, Case Western Reserve University, University of Chicago, Drexel University, Fermilab, the Institute for Advanced Study, the Japan Participation Group, Johns Hopkins University, the Joint Institute for Nuclear Astrophysics, the Kavli Institute for Particle Astrophysics and Cosmology, the Korean Scientist Group, the Chinese Academy of Sciences (LAMOST), Los Alamos National Laboratory, the Max-Planck-Institute for Astronomy (MPA), the Max-Planck-Institute for Astrophysics (MPIA), New Mexico State University, Ohio State University, University of Pittsburgh, University of Portsmouth, Princeton University, the United States Naval Observatory, and the University of Washington.

This publication makes use of data products of the Two Micron All Sky Survey, which is a joint project of the University of Massachusetts and the Infrared Processing and Analysis Center/California Institute of Technology, funded by the National Aeronautics and Space Administration and the National Science Foundation.

Facilities: SDSS, 2MASS

## REFERENCES

Abazajian, K., et al. 2003, AJ, 126, 2081 AJ, 129, 1755

Babusiaux, G. & Gilmore, G. 2005, in “Resolved Stellar Populations”, ASP Conf. Series., eds. D. Valls-Gabaud & M. Chavez ([astro-ph/0506413](http://astro-ph/0506413)).

- Baraffe, I. et al. 1998, A&A, 337, 403 (BCAH98)
- Briceño, C. et al. 2005, AJ, 129, 907
- Briceño, C. et al. 2005, Star Formation in the Era of the Three Great Observatories, July 13-15, Cambridge, MA.
- Cardelli, J. A., Clayton, G .C. & Mathis. J. S. 1989, ApJ, 345, 245
- Finkbeiner, D. et al. 2004, AJ, 128, 2577
- Fukugita, M. et al. 1996, AJ, 111, 1748
- Gunn, J. E. et al. 1998, AJ, 116, 3040
- Gunn, J. E. et al. 2006, AJ, *submitted*, *astro-ph/0602326*.
- Haisch, K E. et al. 2001, AJ, 121, 1512
- Herbst, W. et al. 1994, AJ, 108, 1906
- Hogg, D.W., Finkbeiner, D.P., Schlegel, D.J., & Gunn, J.E. 2001, AJ, 122, 2129
- Ivezić, Ž, Lupton, R.H., Schlegel, D. et al. 2004, AN, 325, No. 6-8, 583-9.
- Johnson, H.L. & Morgan, W.W. 1953, ApJ, 117, 313
- Kenyon, S. J. & Hartmann, L. 1995, ApJS, 101, 117
- Lada, E.A. et al., ApJ, 371, 171
- Liu, M., Najita, J, & Tokunaga, A. 2003, ApJ, 585, 372
- Luhman, K.L. et al. 2003, ApJ, 593, 1093
- Lupton, R.H., Gunn, J.E., & Szalay, A.S. 1999, AJ, 118, 1406
- Lynds, B. T. 1962, ApJS, 7, 1
- Kharchenko, N.V. 2001, Kinematics and Physics of Celestial Bodies, 17, 409
- Kharchenko, N.V., Piskunov, A.E., Roeser, S., Schilbach, E., Scholz, R.-D. 2005, A&A, 440, 403
- McGehee, P.M., West, A.A., Smith, J.A., Anderson, K.S.J., Brinkmann, J. 2005, AJ, 130, 1752

- Meyer, M. R., Calvet, N., & Hillenbrand, L. A. 1997, AJ, 114, 288
- Motte, F. et al. 2001, A&A, 372, L41
- Pier, J.R., Munn, J.A., Hindsley, R.B., Hennessy, G.S., Kent, S.M., Lupton, R.H., & Ivezić, Ž. 2003, AJ, 125, 1559
- Schlegel, D. J., Finkbeiner, D. P., & Davis, M. 1998, ApJ, 500, 525
- Skrutskie, M. F, et al., 1997, The Impact of Large-Scale Near-IR Sky Surveys, F. Garzon et al., eds (Dordrecht:Kluwer)
- Smith, J.A., et al. 2002, AJ, 123, 2121
- Stoughton, C., et al. 2002, AJ, 123, 485
- van den Bergh, S. 2005, *astro-ph/0511702*
- York, D. G. et al. 2000, AJ, 120, 1579

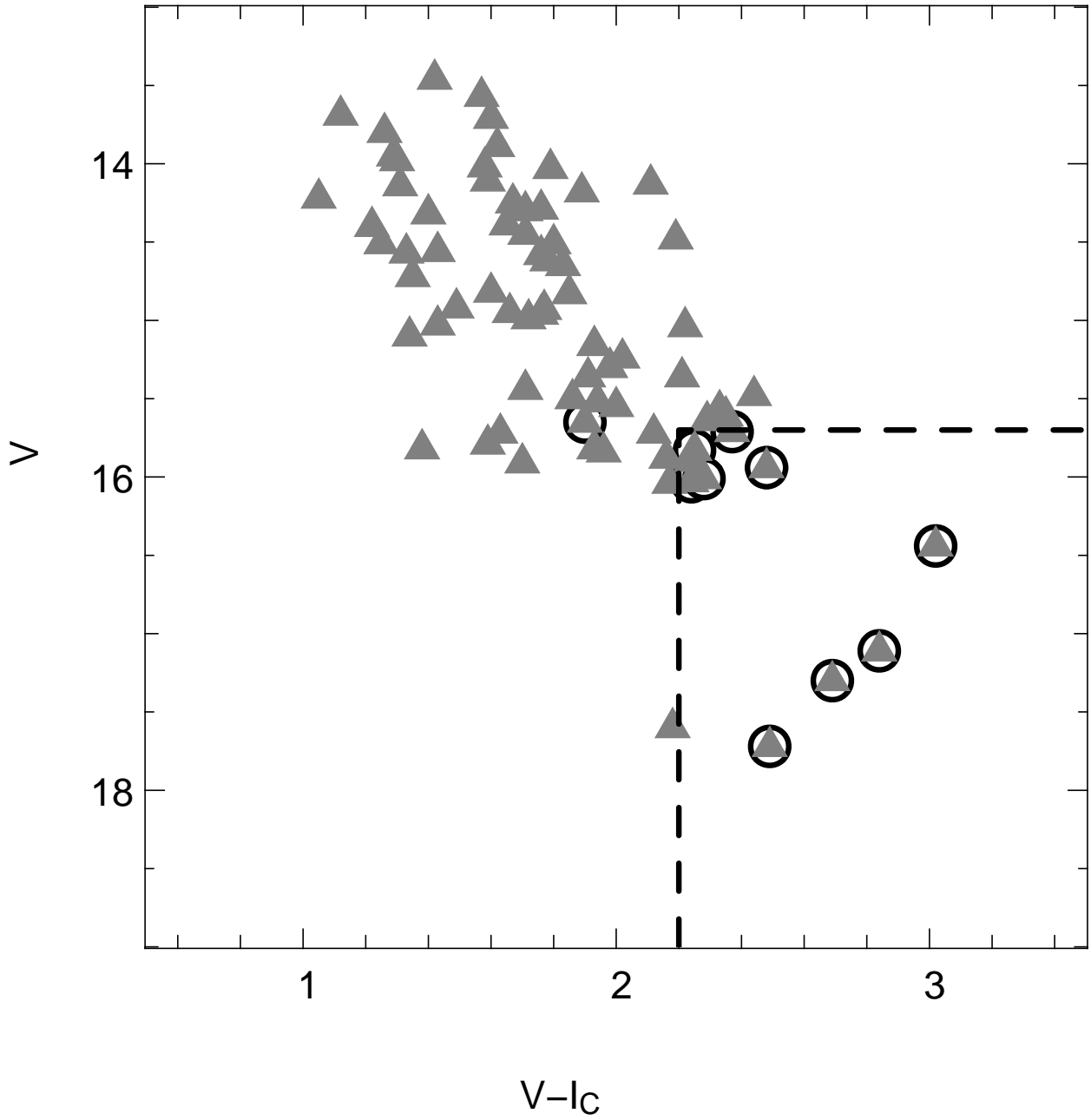


Fig. 1.—  $(V - I_c, V)$  color-magnitude diagram for equatorial CIDA objects. The colors and magnitudes of the 76 spectroscopically confirmed pre-main-sequence objects found in the CIDA Orion Variability Survey that lie within the SDSS equatorial scans are shown here. Those objects selected by the SDSS-based low-mass star study of McGehee et al. (2005) are highlighted by open circles. The effective selection region of the SDSS study is bounded by  $V - I_C > 2.2$  and  $V > 15.7$  (*dashed lines*). The faint star at  $V - I_C = 2.18$ ,  $V = 17.60$  is the continuum CTTS CVS 157.

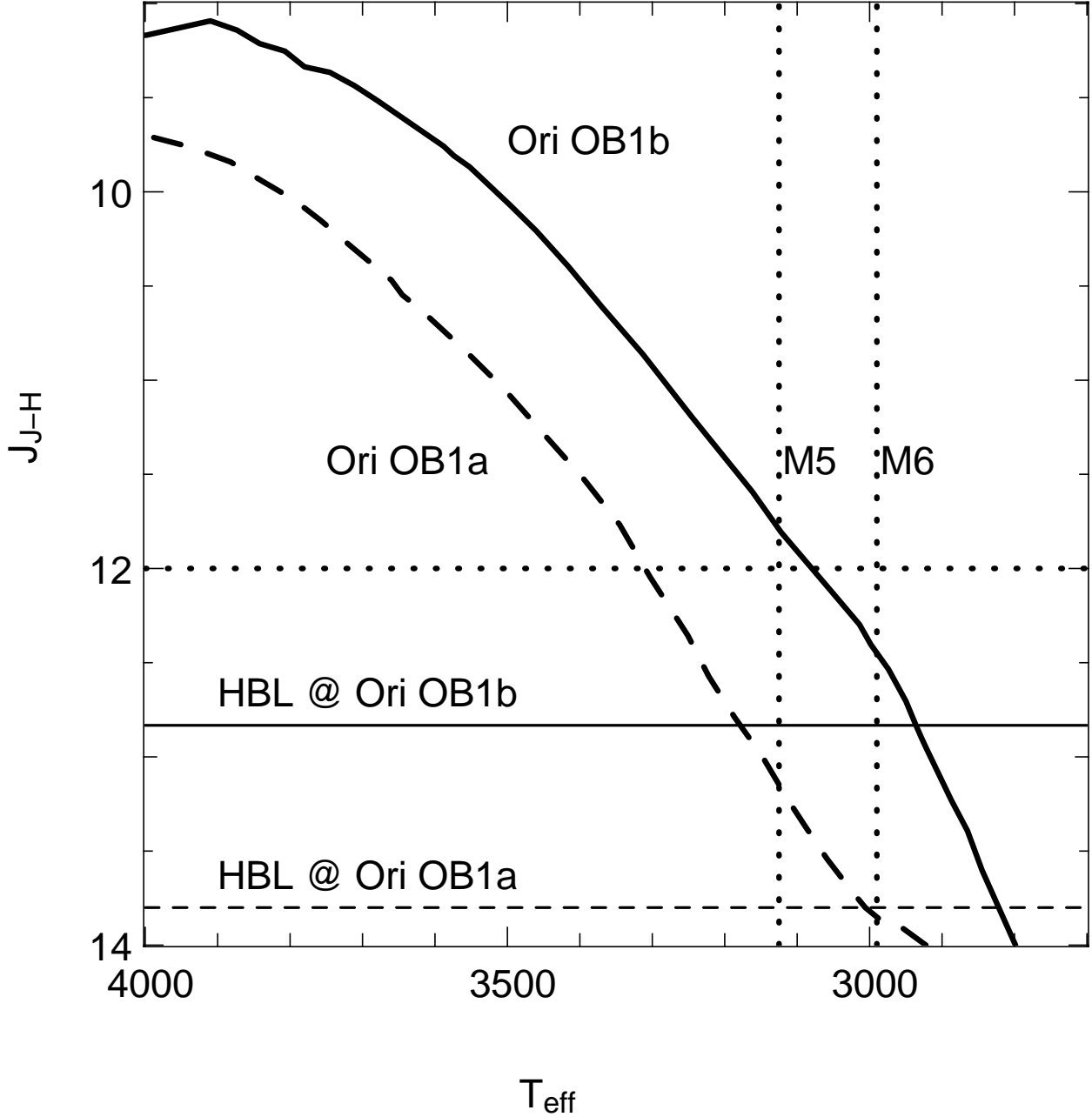


Fig. 2.— ( $J_{J-H}, T_{\text{eff}}$ ) diagram for Orion OB1a and OB1b. The relation between  $T_{\text{eff}}$  and  $J_{J-H}$  for the Orion OB1a (dashed line) and Orion OB1a (solid line) subassociations are shown here based on the BCAH98 models. The two vertical dotted lines mark spectral types of M5 and M6, assuming the PMS temperature scale of Luhman (2003). The faint magnitude limit of  $J_{J-H} = 12.0$  for detection of circumstellar disk signatures, based on a lack of contrast in the NIR for spectral types of M6 or later, is traced by the horizontal dotted line. The Hydrogen Burning Limit ( $0.075 M_{\odot}$ ) is indicated for both subassociations.

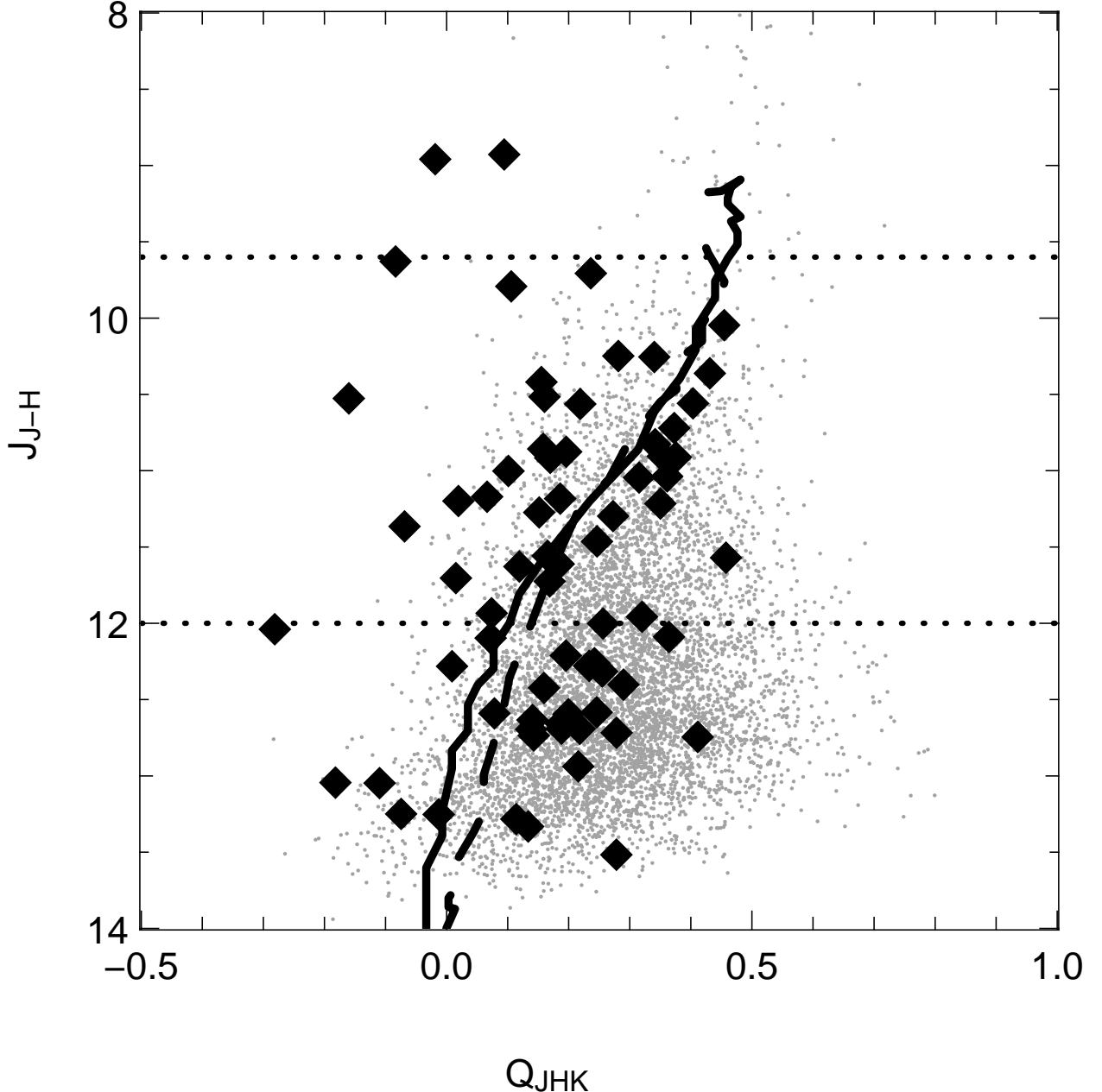


Fig. 3.— **Near-IR color-magnitude diagram for Orion.** The reddening-invariant ( $Q_{JHK}, J_{J-H}$ ) color-magnitude diagram for the Orion sample is plotted here with the BCAH98 isochrones for Orion OB1a (dashed line) and Orion OB1b (solid line) shown as references. The reddening-invariant near-IR excess,  $\Delta Q_{JHK}$ , is measured relative to the isochrones for stars having  $9.6 < J_{J-H} < 12.0$  (dotted lines). Disk candidates ( $\Delta Q_{JHK} < 0$ ) are found to the left of the isochrones. The CTTS candidates, as inferred by SDSS multi-band variability (see Figures 4 and 5), are highlighted by diamonds.

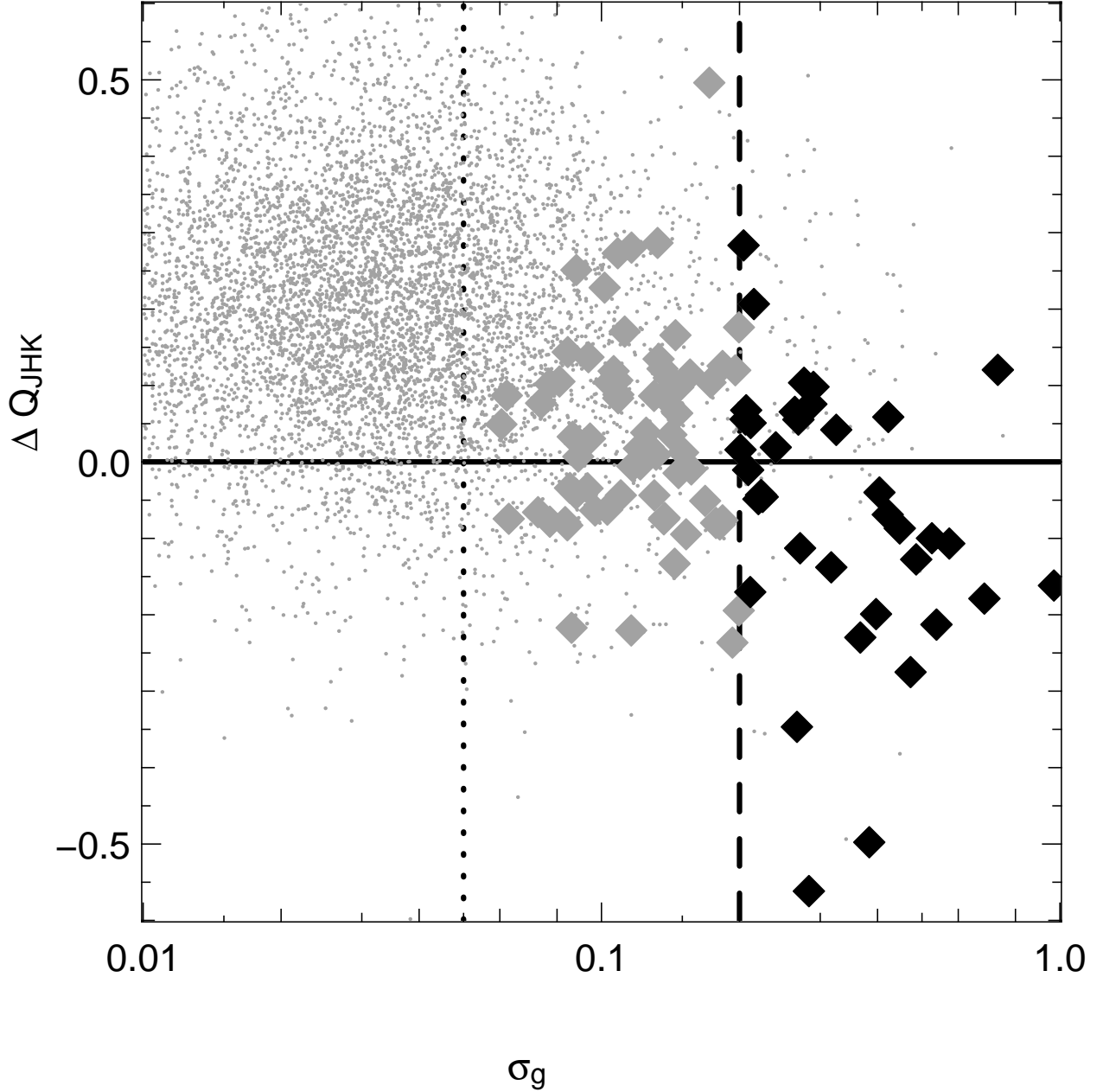


Fig. 4.— **Near-IR excess and  $g$  band variability.** In this figure we compare the intrinsic near-IR excess, as inferred by  $\Delta Q_{JHK}$ , and  $\sigma_g$ , the standard deviation in the  $g$  band measured over all observations of a star. Stars meeting the variability thresholds of McGehee et al. (2005) for CTTS candidates ( $\sigma_g > 0.05$  (dotted line) and  $\sigma_z > 0.05$ ) having  $9.6 < J_{J-H} < 12.0$  (see Figure 3) are shown as diamonds. In this work we increase the  $\sigma_g$  threshold to 0.2 magnitudes (dashed line) due to the marked increase in near-IR excess at this variability level and above. The stars meeting the new variability criteria of  $\sigma_g > 0.2$  and  $\sigma_z > 0.05$  are shown as black diamonds.

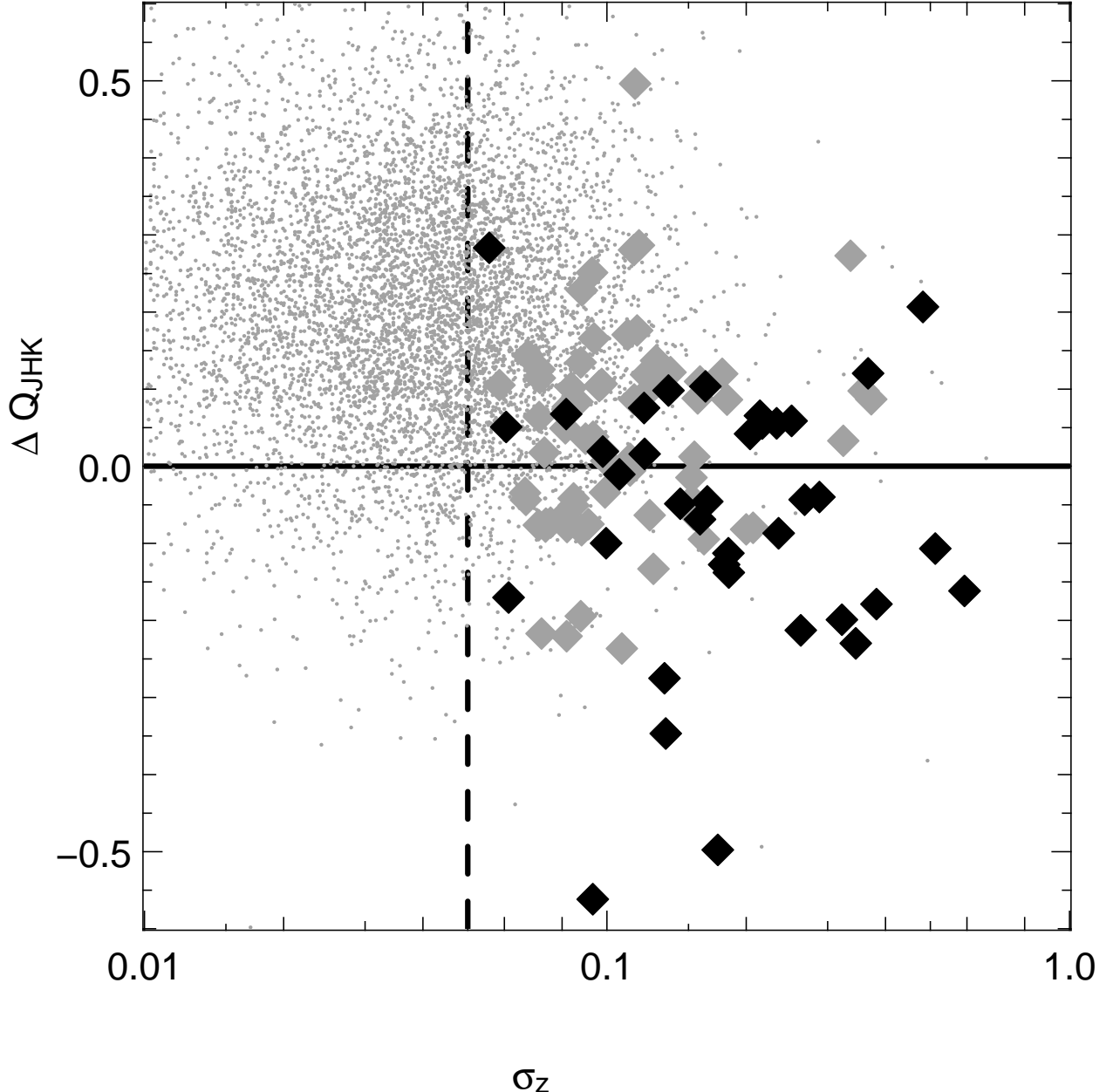


Fig. 5.— **Near-IR excess and  $z$  band variability.** Following Figure 4, we compare the intrinsic near-IR excess, as indicated by  $\Delta Q_{JHK}$ , and  $\sigma_z$ , the standard deviation in the  $z$  band measured over all observations of a star. The  $\sigma_z = 0.05$  threshold used by McGehee et al. (2005) and this work is marked by the dashed line. As in Figure 4 the diamonds indicate CTTS candidates based on the criteria in McGehee et al. (2005) (grey) and this work (black).

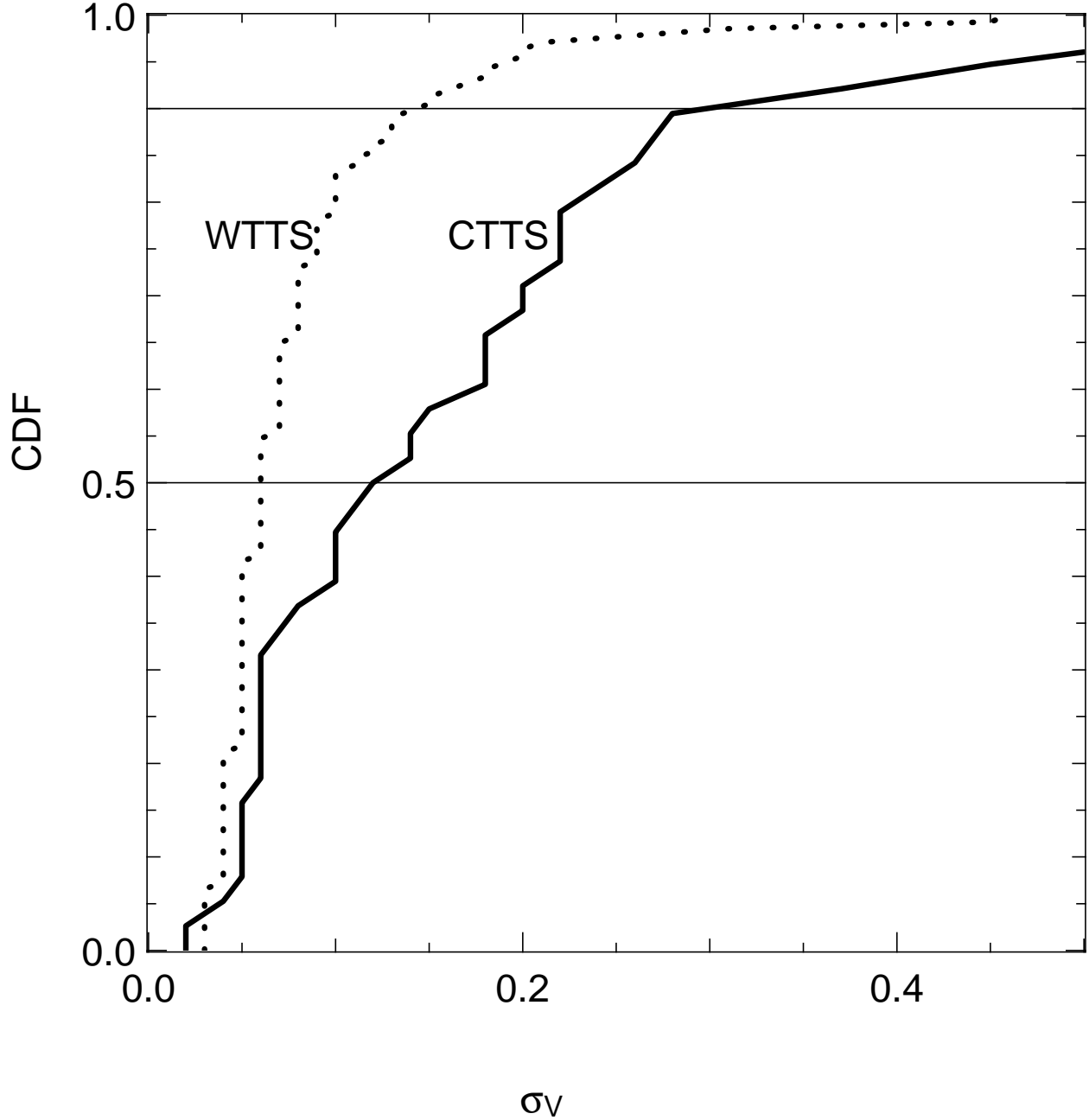


Fig. 6.—  $\sigma_V$  Cumulative Distribution Functions for WTTS and CTTS. The Cumulative Distribution Functions (CDF) of  $\sigma_V$  are shown here for the spectroscopically confirmed WTTS (dotted line) and CTTS (solid line) from Briceño et al. (2005b) where it is clear that the CTTS are much more highly variable than the WTTS. The median value of  $\sigma_V$ , at CDF = 0.5, for the WTTS and CTTS are 0.06 and 0.12 magnitudes, respectively. The 90th percentile values of  $\sigma_V$  for the WTTS and CTTS have a greater spread of 0.14 magnitudes.

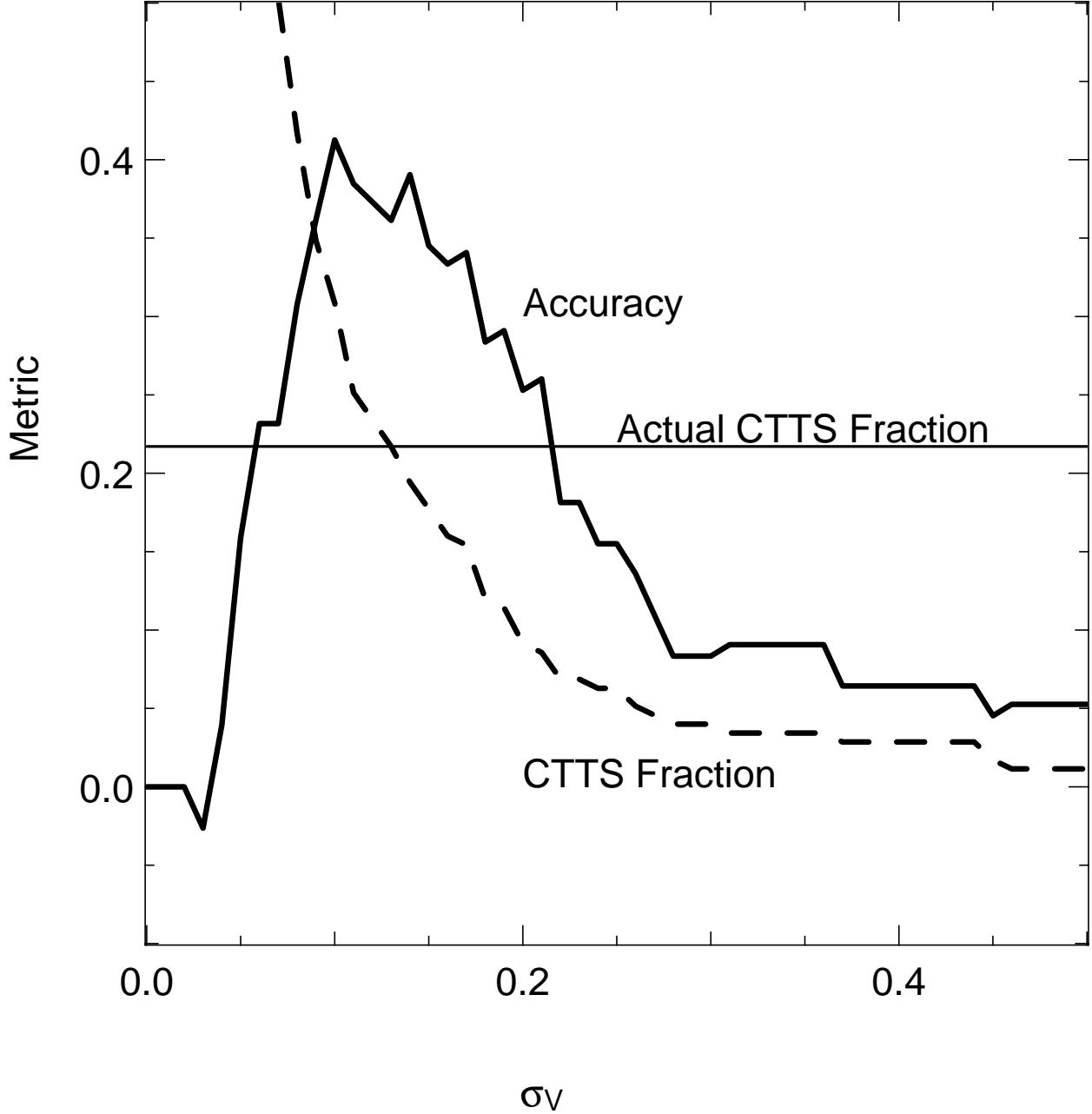


Fig. 7.— **Selection metrics for CTTS classification.** Two selection metrics for CTTS/WTTS discriminations based on a threshold  $\sigma_V$  value are compared here. To assess the ability to correctly identify individual objects we plot the accuracy against the threshold (*solid line*). The dashed line shows the computed CTTS fraction (*dashed line*) which is compared against the actual value in the sample (*horizontal line*). Both selection metrics give their best performance for  $0.10 < \sigma_V < 0.15$ .

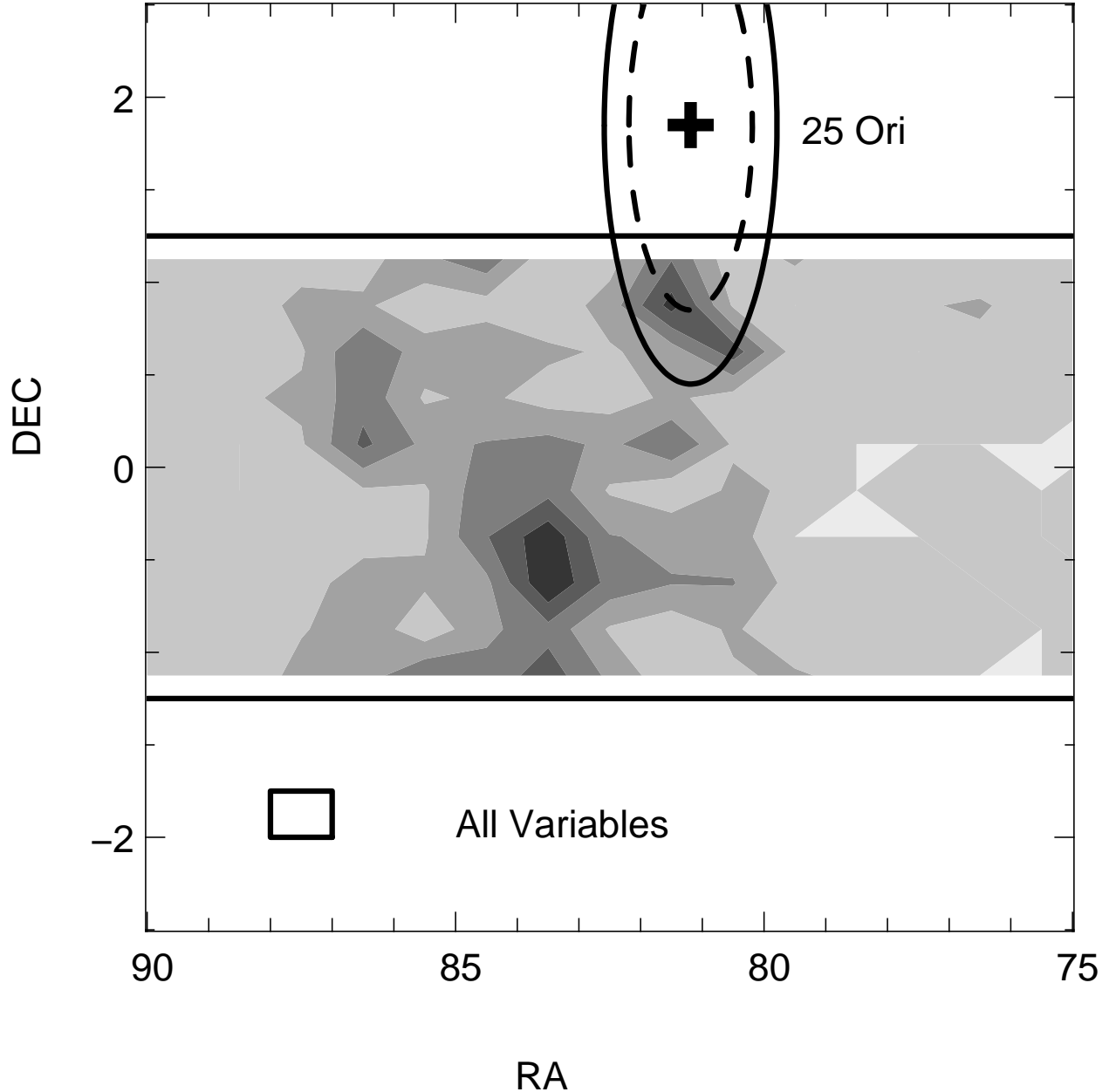


Fig. 8.— **Stellar densities.** The surface densities of PMS candidates selected by variability ( $\sigma_g > 0.05$ ) are presented here. The densities are computed based on  $1.0^\circ$  by  $0.25^\circ$  regions (see box in lower left) with the contours uniformly spaced between 0.0 stars  $\text{deg}^{-2}$  and a maximum of 68 stars  $\text{deg}^{-2}$ . The L1630 complex ( $\alpha_{2000} = 86.5^\circ$ ), Orion OB1b subassociation, and the 25 Ori group are evident. The circles of radii  $1.0^\circ$  and  $1.4^\circ$  are centered on the Be star 25 Orionis (*cross*) and mark the approximate extent of the 25 Ori group.

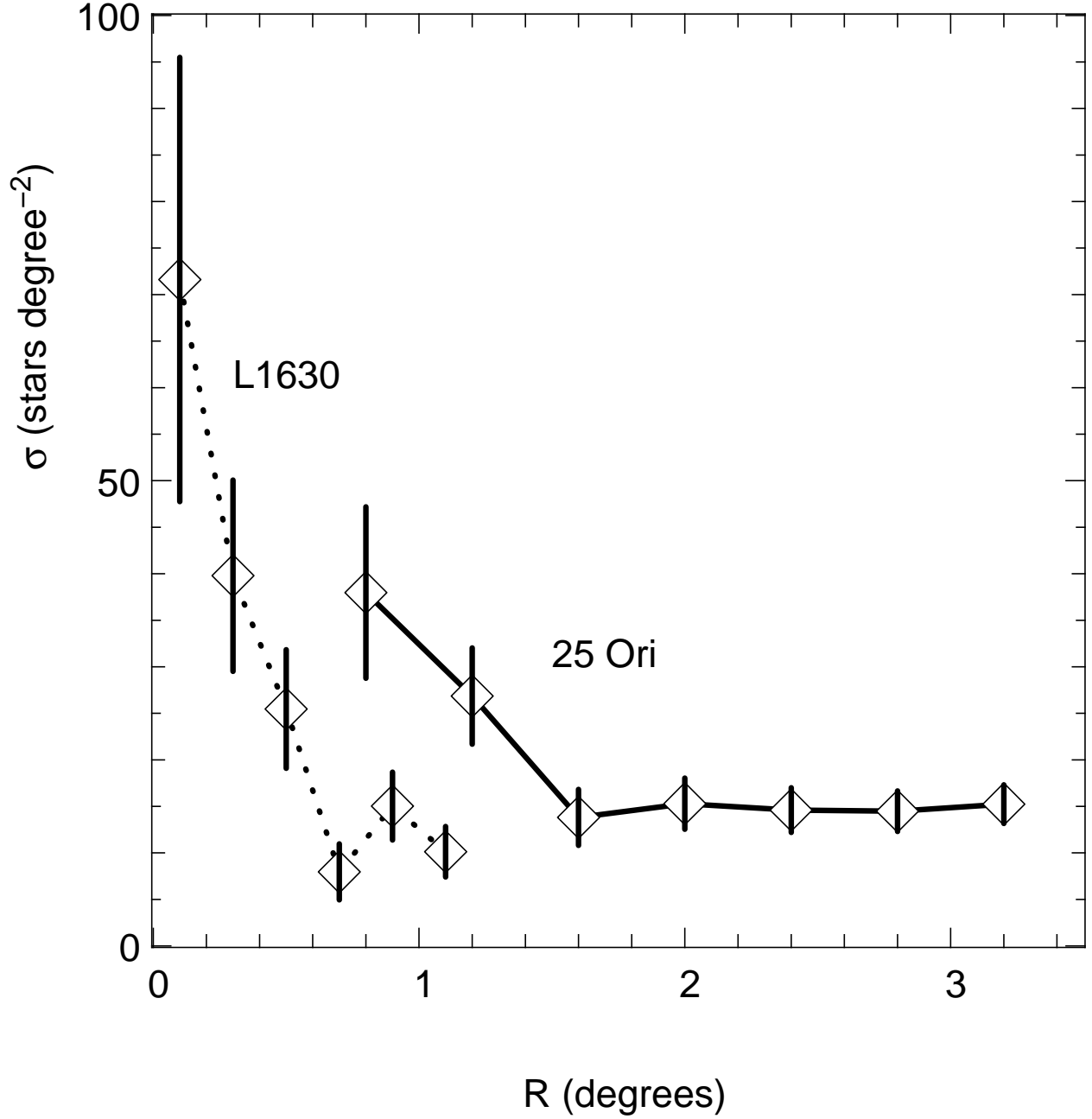


Fig. 9.— **Stellar density versus distance from group center.** The signatures of the 25 Ori group (*solid line*) and the NGC 2068/NGC 2071 active star formation site in L1630 (*dotted line*) are evident in this plot of the surface density of SDSS PMS candidates using radial bins. Spacings of  $0.4^\circ$  and  $0.2^\circ$  are used for the 25 Ori and L1630 regions, respectively. The innermost bin for the 25 Ori group spans distances of  $0.6^\circ$  to  $1.0^\circ$ . We estimate the outer radius of the 25 Ori group as  $1.4^\circ$  and that of the northern L1630 protocluster as  $0.6^\circ$ . The  $\pm 1\sigma$  error bars are computed based on Poisson statistics.

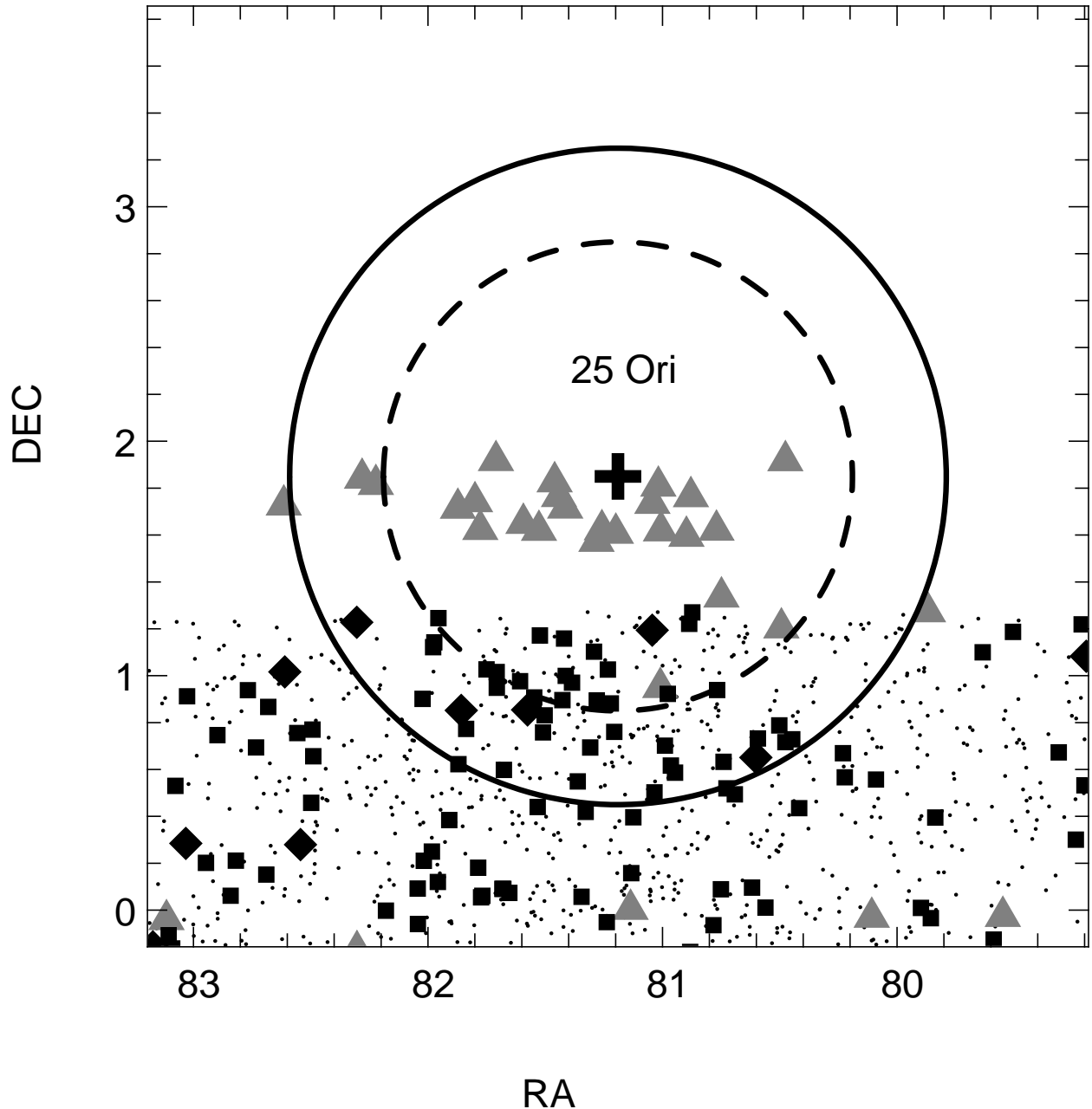


Fig. 10.— **The 25 Ori Region.** In this figure we show the locations in equatorial coordinates of the spectroscopically confirmed T Tauris from the CIDA Variability Survey of Orion (*grey triangles*), SDSS WTTS candidates (*small squares*), and SDSS CTTS candidates (*diamonds*) within 2 degrees of 25 Ori. The circles of radii  $1.0^{\circ}$  and  $1.4^{\circ}$  are centered on the Be star 25 Ori (*cross*) and mark the approximate extent of the 25 Ori group. The candidate low-mass stars observed for least 2 epochs by the SDSS are shown as points.

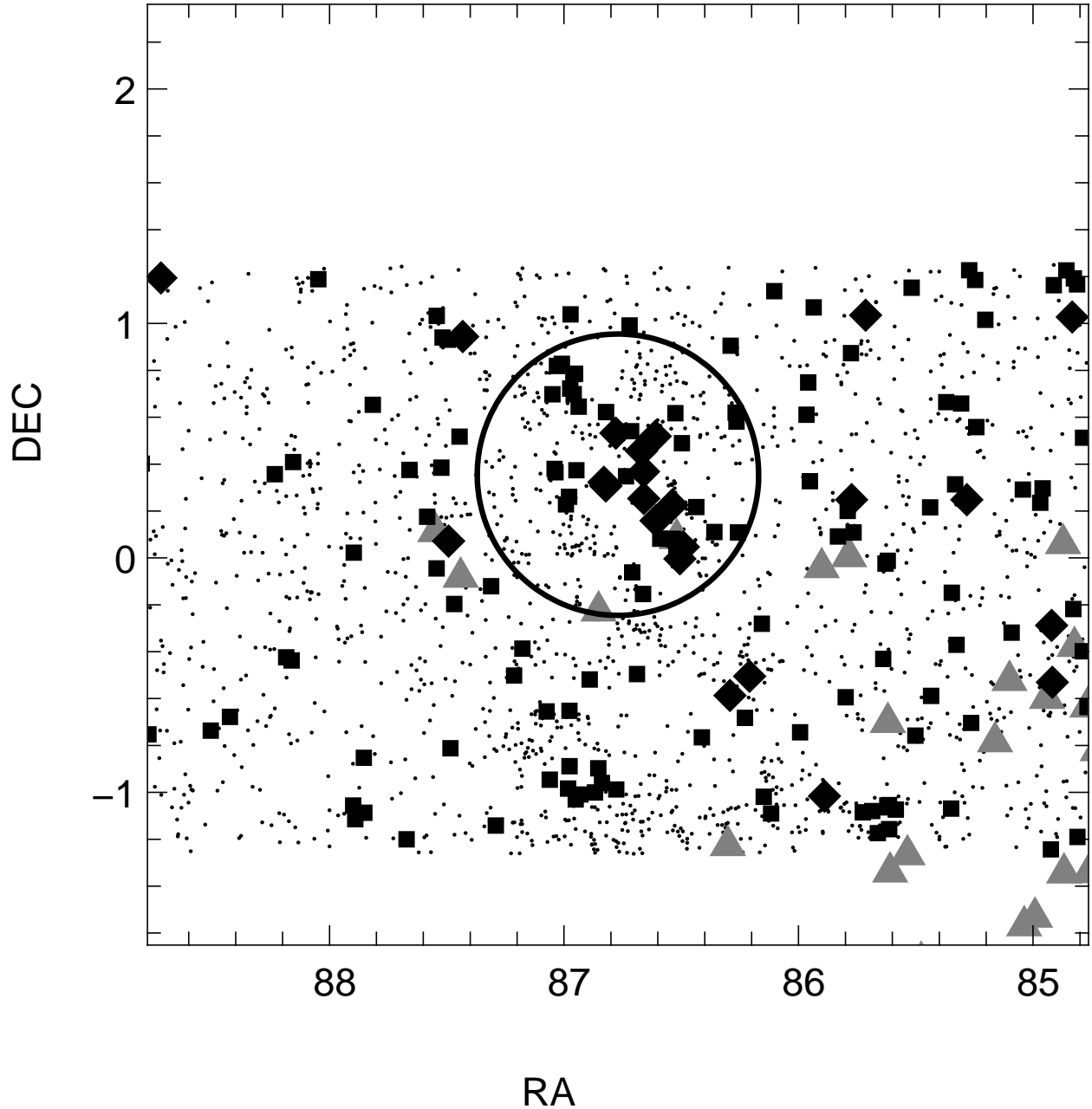


Fig. 11.— **The NGC 2068/NGC 2071 region.** In this figure we show the locations in equatorial coordinates of the spectroscopically confirmed T Tauris from the CIDA Variability Survey of Orion (*grey triangles*), SDSS WTTS candidates (*small squares*), and SDSS CTTS candidates (*diamonds*) within 2 degrees of NGC 2071. The circle centered on NGC 2071 has a radius  $0.6^\circ$ . The candidate low-mass stars observed for least 2 epochs by the SDSS are shown as points.

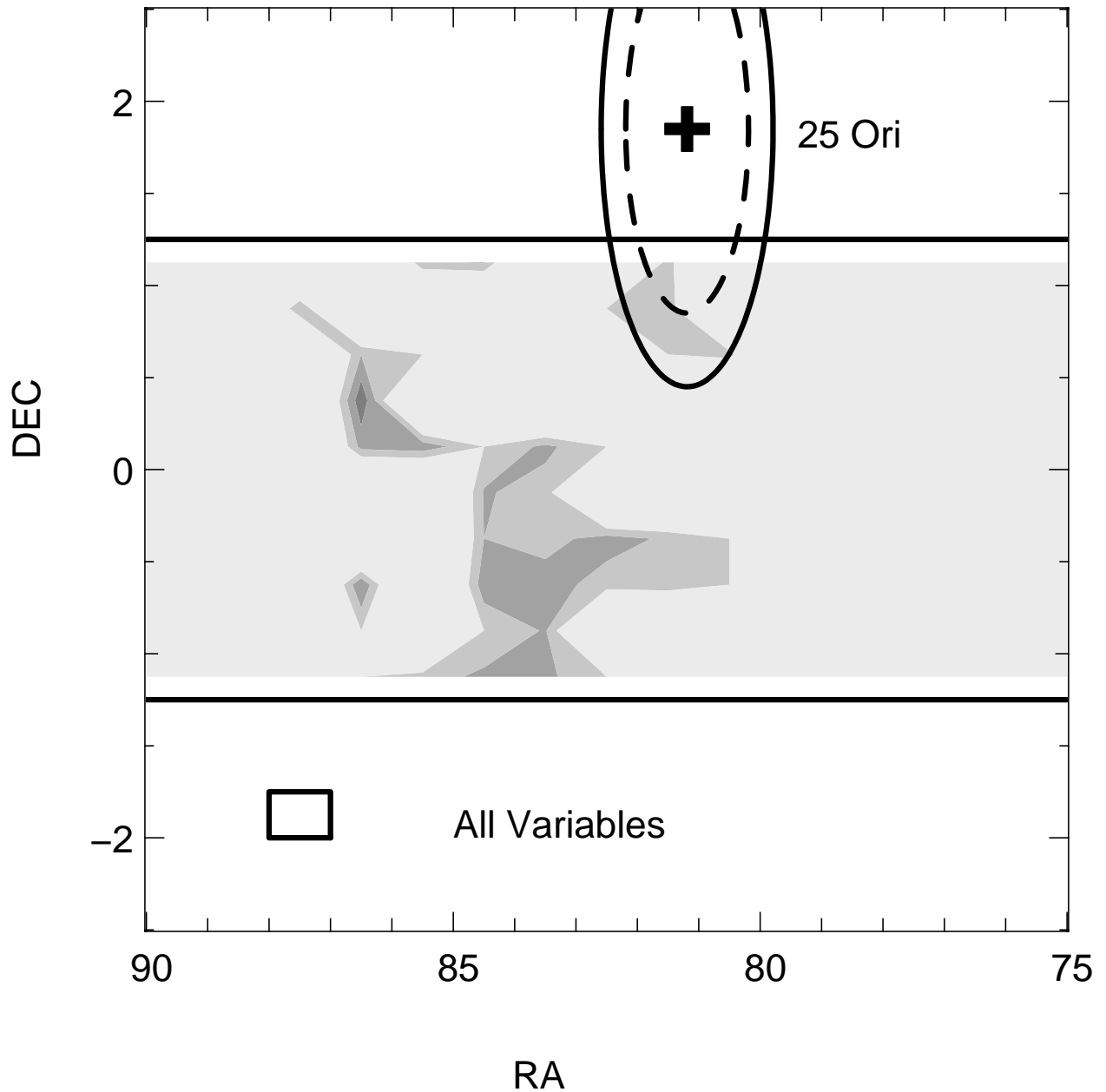


Fig. 12.— **CTTS fractions.** The fraction of CTTS candidates, is shown here using the same samples and gridding as define in Figure 8. The contours are uniformly spaced between 0.0 and 1.0. Both the L1630 complex and the Orion OB1b subassociation have relatively high CTTS fractions.

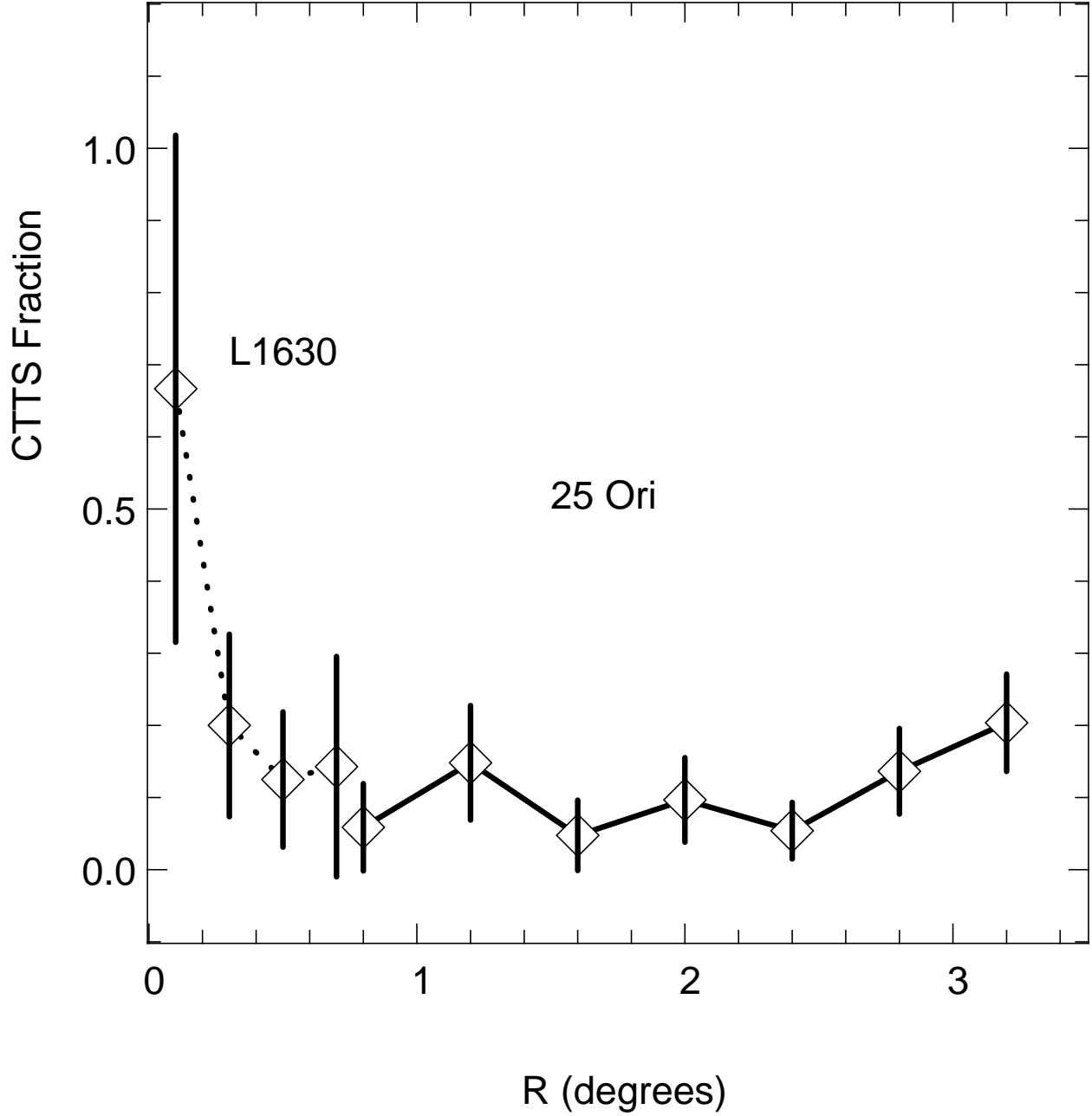


Fig. 13.— **CTTS fraction versus distance from group center.** The 25 Ori group has a mean CTTS fraction (*solid line*) as  $\sim 0.1$ , as seen in this plot of CTTS fraction against radial distance from 25 Orionis. This fraction is identical to that observed in the Orion OB1a field surrounding the 25 Ori group. In contrast, the central region of NGC 2068/NGC 2071 protocluster (*dotted line*) has a high CTTS fraction of  $\sim 0.7$ . The CTTS fractions are computed using the same radial bins as in Figure 9. The  $\pm 1\sigma$  error bars are computed based on Poisson statistics.

Table 1. Matches between the SDSS and CVSO Surveys

CVSO	SDSS Name	<i>g</i>	<i>r</i>	<i>i</i>	<i>z</i>	R <sup>a</sup>	Class <sup>b</sup>	Confirmed	Class <sup>c</sup>
CVSO 1	SDSS J051058.78-000803.1	17.96	16.58	15.12	14.33	3.98	W	C	
CVSO 13	SDSS J052242.82-005306.5	17.17	15.71	14.70	14.07	2.78	W	W	
CVSO 49	SDSS J052806.91-001806.0	18.47	17.06	15.74	14.98	2.31	W	W	
CVSO 81	SDSS J053055.62-005540.0	17.02	15.69	14.51	13.74	3.18	-	W	
CVSO 124	SDSS J053349.04-004625.9	16.81	15.44	14.29	13.63	3.47	W	W	
CVSO 142	SDSS J053530.03-002822.7	17.04	15.60	14.48	13.93	3.55	-	W	
CVSO 156	SDSS J053747.02-002007.2	16.73	15.38	14.25	13.50	3.92	-	C	
CVSO 162	SDSS J053830.84-011024.3	16.74	15.36	14.51	14.05	4.58	-	W	
CVSO 164	SDSS J053853.84-004920.0	17.51	16.14	14.64	13.56	4.43	W	C	
CVSO 168	SDSS J053904.29-003810.0	18.19	16.76	15.34	14.48	4.36	W	W	

<sup>a</sup>Distance in degrees from the Be star 25 Orionis.

<sup>b</sup>Preliminary classification as not PMS (-), WTTS (W) or CTTS (C) based on multi-band variability.

<sup>c</sup>Classification as WTTS (W) or CTTS (C) on the basis of optical spectroscopy (Briceño et al. 2005b).

Table 2. Candidate Low-Mass PMS in the Orion Equatorial Region

Name	RA	DEC	<i>g</i>	<i>r</i>	<i>i</i>	<i>z</i>	R <sup>b</sup>	Class <sup>c</sup>
SDSS J050013.47+011349.1	75.0562	1.2303	19.90	18.24	16.67	15.77	6.17	W
SDSS J050013.86+005807.4	75.0578	0.9687	16.85	15.44	14.57	14.09	6.20	W
SDSS J050058.65+002106.9	75.2444	0.3519	19.92	18.29	16.14	15.03	6.13	W
SDSS J050333.53-004138.2	75.8897	-0.6940	18.79	17.40	15.84	14.96	5.88	W
SDSS J050531.61+002616.3	76.3817	0.4379	20.56	18.78	16.82	15.88	5.01	W
SDSS J050548.68-000332.8	76.4528	-0.0591	19.06	17.33	16.35	15.86	5.11	W
SDSS J050549.25+005120.9	76.4552	0.8558	19.22	17.54	16.50	15.94	4.84	W
SDSS J050601.35-004831.0	76.5057	-0.8086	18.14	16.56	15.93	15.64	5.39	W
SDSS J050606.25+004226.5	76.5261	0.7074	18.65	17.05	15.85	15.28	4.80	W
SDSS J050611.43+004053.3	76.5476	0.6815	19.64	18.09	16.87	16.29	4.79	W
SDSS J050613.73+001627.2	76.5572	0.2742	18.58	17.03	15.98	15.47	4.89	W
SDSS J050627.87-002129.1	76.6162	-0.3581	17.66	16.26	15.12	14.45	5.08	W
SDSS J050633.48+004747.3	76.6395	0.7965	19.25	17.70	16.50	15.88	4.67	W
SDSS J050635.51-005531.6	76.6480	-0.9255	18.83	17.32	15.86	15.11	5.32	W
SDSS J050639.89-004913.1	76.6662	-0.8203	16.27	14.70	13.38	12.74	5.25	W
SDSS J050648.67+001748.6	76.7028	0.2968	18.93	17.30	16.16	15.73	4.75	W
SDSS J050649.68-000917.4	76.7070	-0.1549	18.07	16.64	15.49	14.92	4.91	W
SDSS J050651.84+004813.6	76.7160	0.8038	18.99	17.45	16.34	15.81	4.59	W
SDSS J050750.43+005414.9	76.9602	0.9042	18.44	17.07	15.79	15.11	4.33	W
SDSS J050909.42+001512.5	77.2893	0.2535	18.58	17.26	16.27	15.78	4.21	C
SDSS J050910.93-005715.4	77.2956	-0.9543	18.30	16.89	15.59	14.85	4.80	W
SDSS J050939.12-003739.0	77.4130	-0.6275	18.35	16.83	15.51	14.59	4.52	W
SDSS J051037.47+004943.4	77.6561	0.8287	17.61	16.59	15.32	14.99	3.68	W
SDSS J051052.52-003700.4	77.7188	-0.6168	19.47	18.28	16.95	16.03	4.26	C
SDSS J051058.78-000803.1	77.7449	-0.1342	17.96	16.58	15.12	14.33	3.98	W
SDSS J051107.89+005450.4	77.7829	0.9140	19.54	18.11	16.75	16.00	3.53	W
SDSS J051112.40+005645.5	77.8017	0.9460	17.29	15.88	14.23	13.27	3.51	W
SDSS J051142.74+010149.1	77.9281	1.0303	18.42	17.04	15.72	15.00	3.36	W
SDSS J051232.90-003851.5	78.1371	-0.6477	19.79	18.35	16.90	16.02	3.94	W
SDSS J051313.77+001702.9	78.3074	0.2842	18.27	16.87	15.65	15.03	3.28	W
SDSS J051347.73+005505.5	78.4489	0.9182	16.87	15.36	14.22	13.59	2.90	W
SDSS J051351.57-011337.3	78.4649	-1.2270	16.78	15.39	14.24	13.62	4.11	W
SDSS J051445.52+004416.1	78.6897	0.7378	19.29	17.63	16.38	15.78	2.74	W
SDSS J051454.97+004640.2	78.7291	0.7779	18.65	17.01	15.72	15.07	2.68	W
SDSS J051515.78-010006.4	78.8158	-1.0018	19.24	17.66	16.75	16.22	3.71	W
SDSS J051518.75+004333.4	78.8281	0.7260	16.84	15.29	14.59	14.26	2.62	W
SDSS J051646.31+010458.7	79.1930	1.0830	19.92	18.54	17.13	16.33	2.14	C
SDSS J051648.18+003155.9	79.2008	0.5322	17.86	16.41	15.33	14.74	2.39	W
SDSS J051651.05+011308.1	79.2127	1.2189	18.51	17.15	15.69	14.88	2.08	W
SDSS J051657.06+001802.0	79.2378	0.3006	19.83	18.37	16.52	15.55	2.49	W
SDSS J051714.49+004023.1	79.3104	0.6731	17.84	16.42	14.95	14.23	2.22	W
SDSS J051755.36-003912.7	79.4807	-0.6535	17.68	16.25	15.15	14.51	3.03	C
SDSS J051801.35+011112.1	79.5057	1.1867	17.88	16.46	15.50	15.03	1.81	W
SDSS J051809.05-001230.7	79.5377	-0.2086	19.33	17.93	16.39	15.59	2.64	W
SDSS J051821.11-000733.6	79.5880	-0.1260	17.80	16.38	15.20	14.51	2.54	W
SDSS J051822.37-010511.0	79.5932	-1.0864	19.03	17.57	16.04	15.15	3.34	W

Table 2—Continued

Name	RA	DEC	<i>g</i>	<i>r</i>	<i>i</i>	<i>z</i>	R <sup>b</sup>	Class <sup>c</sup>
SDSS J051832.38+010559.4	79.6349	1.0998	18.14	16.66	15.72	15.17	1.73	W
SDSS J051858.70-003815.6	79.7446	-0.6377	18.78	17.35	15.90	14.94	2.88	W
SDSS J051912.02-010514.9	79.8001	-1.0875	17.15	15.75	14.79	14.26	3.25	C
SDSS J051920.84+002341.3	79.8369	0.3948	17.26	15.86	14.82	14.26	1.99	W
SDSS J051925.42-000203.0	79.8560	-0.0342	19.16	17.91	16.55	15.89	2.31	W
SDSS J051926.99-011157.1	79.8625	-1.1992	20.45	18.97	17.43	16.53	3.33	C
SDSS J051935.47+000035.0	79.8978	0.0097	18.65	17.18	16.32	15.91	2.25	W
SDSS J051947.40-011420.6	79.9475	-1.2391	19.82	18.32	16.67	15.73	3.33	W
SDSS J052015.55-001922.2	80.0648	-0.3229	21.37	19.86	17.89	16.79	2.45	W
SDSS J052021.54+003325.1	80.0898	0.5570	19.79	18.38	17.11	16.37	1.70	W
SDSS J052024.03-004631.9	80.1001	-0.7755	19.22	17.79	16.23	15.20	2.84	W
SDSS J052033.20-004330.2	80.1384	-0.7251	19.37	17.94	16.53	15.78	2.78	W
SDSS J052042.36-001723.9	80.1765	-0.2900	19.60	18.13	16.94	16.28	2.37	W
SDSS J052042.75-004309.6	80.1781	-0.7194	18.90	17.37	15.94	15.01	2.76	W
SDSS J052047.14-004840.3	80.1964	-0.8112	18.37	16.85	16.11	15.78	2.84	W
SDSS J052053.45+003359.3	80.2227	0.5665	17.83	16.43	15.22	14.54	1.61	W
SDSS J052055.35+004009.8	80.2307	0.6694	19.17	17.66	15.89	14.93	1.52	W
SDSS J052139.86-004454.2	80.4161	-0.7484	18.39	16.88	15.55	14.77	2.71	W
SDSS J052140.09+002605.9	80.4171	0.4350	17.88	16.46	15.29	14.63	1.61	W
SDSS J052147.21+004343.0	80.4467	0.7286	16.36	14.92	14.17	13.89	1.35	W
SDSS J052154.25+004259.3	80.4761	0.7165	18.53	17.10	15.99	15.52	1.34	W
SDSS J052154.83-004323.3	80.4785	-0.7231	18.13	16.68	15.57	14.91	2.67	W
SDSS J052200.52+004716.3	80.5022	0.7879	20.26	18.67	17.18	16.36	1.27	W
SDSS J052214.62+000039.5	80.5610	0.0110	17.84	16.31	15.47	15.06	1.94	W
SDSS J052217.23-001611.0	80.5718	-0.2697	18.03	16.63	15.55	14.94	2.21	W
SDSS J052222.44+004356.4	80.5935	0.7323	18.09	16.61	15.18	14.46	1.27	W
SDSS J052224.45+003903.7	80.6019	0.6511	19.84	18.35	16.65	15.80	1.34	C
SDSS J052224.91-001708.7	80.6038	-0.2858	19.03	17.59	16.57	16.04	2.21	W
SDSS J052228.40+000546.0	80.6183	0.0961	18.01	16.53	15.78	15.41	1.84	W
SDSS J052230.85-001235.5	80.6286	-0.2099	16.56	15.12	14.20	13.71	2.14	W
SDSS J052235.19-010846.7	80.6466	-1.1463	17.90	16.47	15.26	14.53	3.05	C
SDSS J052242.82-005306.5	80.6784	-0.8851	17.17	15.71	14.70	14.07	2.78	W
SDSS J052245.99+002937.8	80.6916	0.4939	16.74	15.36	14.46	13.95	1.44	W
SDSS J052254.52+003110.3	80.7272	0.5195	19.39	17.98	16.27	15.35	1.41	W
SDSS J052256.90-003343.8	80.7371	-0.5622	19.00	17.60	16.28	15.49	2.45	W
SDSS J052257.49+003757.6	80.7396	0.6327	18.64	17.18	15.64	14.82	1.30	W
SDSS J052300.22+000520.5	80.7509	0.0890	18.07	16.69	15.25	14.52	1.81	W
SDSS J052304.07+005619.9	80.7670	0.9389	18.71	17.28	16.33	15.81	1.00	W
SDSS J052305.37-004007.8	80.7724	-0.6688	17.46	16.04	15.15	14.61	2.55	W
SDSS J052307.82-000351.0	80.7826	-0.0642	19.69	18.24	16.84	16.13	1.96	W
SDSS J052323.30-002713.6	80.8471	-0.4538	17.64	16.20	14.99	14.36	2.33	W
SDSS J052324.18-010319.3	80.8508	-1.0554	18.98	17.49	16.63	16.22	2.93	W
SDSS J052329.50+011612.2	80.8729	1.2701	17.15	15.71	14.53	13.83	0.66	W
SDSS J052331.69-001042.3	80.8821	-0.1784	19.57	18.19	16.53	15.56	2.05	W
SDSS J052332.70+011317.1	80.8863	1.2214	17.43	16.01	14.93	14.36	0.70	W
SDSS J052338.33-001247.6	80.9097	-0.2132	19.61	18.21	16.69	15.77	2.08	W

Table 2—Continued

Name	RA	DEC	<i>g</i>	<i>r</i>	<i>i</i>	<i>z</i>	R <sup>b</sup>	Class <sup>c</sup>
SDSS J052347.15+003510.5	80.9465	0.5863	18.79	17.39	15.89	15.12	1.29	W
SDSS J052348.42-011350.4	80.9518	-1.2307	19.28	17.78	16.10	15.10	3.09	W
SDSS J052351.47+003700.6	80.9645	0.6168	17.74	16.27	15.01	14.40	1.25	W
SDSS J052354.63+005520.8	80.9776	0.9225	16.86	15.44	14.61	14.15	0.95	W
SDSS J052356.59-005814.7	80.9858	-0.9708	17.34	15.92	14.64	13.98	2.83	W
SDSS J052356.65-004223.6	80.9861	-0.7066	18.26	16.90	15.37	14.49	2.56	W
SDSS J052357.49+004206.3	80.9896	0.7018	20.10	18.68	16.97	16.06	1.17	W
SDSS J052403.31-001838.9	81.0138	-0.3108	18.66	17.26	15.99	15.28	2.17	W
SDSS J052408.21+003007.9	81.0342	0.5022	17.63	16.25	15.09	14.48	1.36	W
SDSS J052410.49+011138.0	81.0437	1.1939	17.15	15.80	14.86	14.33	0.67	C
SDSS J052429.84+002345.9	81.1244	0.3961	17.64	16.40	15.16	14.35	1.46	W
SDSS J052432.01+000928.7	81.1334	0.1580	18.30	16.91	15.48	14.76	1.69	W
SDSS J052436.76-004246.7	81.1532	-0.7130	20.04	18.58	16.97	16.07	2.56	W
SDSS J052441.03-002631.4	81.1710	-0.4421	18.53	17.05	15.78	15.07	2.29	W
SDSS J052443.29-002144.6	81.1804	-0.3624	18.77	17.31	16.33	15.77	2.21	W
SDSS J052446.57-001632.1	81.1941	-0.2756	18.65	17.25	15.91	15.15	2.13	W
SDSS J052447.78-003741.4	81.1991	-0.6282	19.41	18.00	16.38	15.49	2.48	W
SDSS J052449.37+004537.3	81.2057	0.7604	17.34	15.77	14.83	14.23	1.09	W
SDSS J052452.91+005254.1	81.2205	0.8817	19.83	18.38	17.03	16.30	0.97	W
SDSS J052455.89+010133.8	81.2329	1.0261	20.90	19.35	17.30	16.18	0.83	W
SDSS J052457.07-000304.1	81.2378	-0.0512	16.83	15.45	14.51	13.96	1.90	W
SDSS J052505.71-003030.7	81.2738	-0.5085	20.48	19.05	17.38	16.37	2.36	C
SDSS J052507.32+005339.5	81.2805	0.8943	19.27	17.84	16.25	15.40	0.96	W
SDSS J052510.11+010608.6	81.2922	1.1024	17.67	16.19	15.06	14.43	0.75	W
SDSS J052513.93+004137.3	81.3081	0.6937	20.53	18.73	16.99	16.11	1.16	W
SDSS J052514.52-005626.6	81.3105	-0.9407	19.57	18.15	16.56	15.65	2.79	W
SDSS J052518.59+002508.9	81.3275	0.4192	18.17	16.67	15.47	14.86	1.44	W
SDSS J052522.85+000325.8	81.3452	0.0572	19.37	17.97	16.47	15.60	1.80	W
SDSS J052526.69+003256.9	81.3612	0.5492	17.42	16.03	14.68	13.95	1.31	W
SDSS J052532.56+005813.0	81.3857	0.9703	17.01	15.59	14.45	13.80	0.90	W
SDSS J052538.97+005957.1	81.4124	0.9992	18.82	17.38	16.43	15.91	0.88	W
SDSS J052540.77+010930.4	81.4199	1.1585	17.80	16.39	15.08	14.30	0.73	W
SDSS J052542.40+005345.2	81.4267	0.8959	18.50	17.11	15.75	15.00	0.98	W
SDSS J052600.63+004951.3	81.5026	0.8309	18.42	17.01	16.14	15.75	1.07	W
SDSS J052600.74-004216.1	81.5031	-0.7045	19.34	17.93	16.38	15.51	2.57	W
SDSS J052602.29+004528.8	81.5096	0.7580	19.37	17.92	16.51	15.83	1.14	W
SDSS J052605.29-004227.5	81.5221	-0.7077	17.57	16.19	15.15	14.55	2.58	W
SDSS J052605.45+011017.1	81.5228	1.1714	16.85	15.53	14.73	14.28	0.76	W
SDSS J052607.74+002624.2	81.5323	0.4401	19.08	17.67	16.10	15.25	1.45	W
SDSS J052610.25-001847.5	81.5427	-0.3132	21.05	19.55	17.69	16.70	2.19	C
SDSS J052610.30-002247.9	81.5429	-0.3800	17.82	16.43	15.35	14.72	2.26	W
SDSS J052611.22+005425.9	81.5468	0.9072	18.87	17.45	16.33	15.72	1.01	W
SDSS J052612.03+005223.9	81.5501	0.8733	20.50	18.95	17.19	16.24	1.04	W
SDSS J052613.73-004347.7	81.5572	-0.7299	19.13	17.63	16.75	16.25	2.61	W
SDSS J052618.12+005114.8	81.5755	0.8541	20.99	19.43	17.74	16.91	1.07	C
SDSS J052625.73+005835.8	81.6072	0.9766	17.29	15.84	14.60	13.88	0.97	W

Table 2—Continued

Name	RA	DEC	<i>g</i>	<i>r</i>	<i>i</i>	<i>z</i>	R <sup>b</sup>	Class <sup>c</sup>
SDSS J052636.70+000424.8	81.6529	0.0736	17.89	16.53	15.05	14.28	1.84	W
SDSS J052642.28+003553.7	81.6762	0.5983	18.89	17.51	16.14	15.37	1.34	W
SDSS J052642.86+000527.7	81.6786	0.0910	18.49	17.13	15.65	14.82	1.83	W
SDSS J052643.92+000526.5	81.6830	0.0907	19.28	17.82	16.36	15.61	1.83	W
SDSS J052649.55+005654.6	81.7065	0.9485	20.02	18.56	16.80	15.89	1.04	W
SDSS J052649.69+010056.2	81.7071	1.0156	17.83	16.42	15.05	14.32	0.98	W
SDSS J052700.12+010136.8	81.7505	1.0269	18.07	16.82	15.52	14.72	1.00	W
SDSS J052704.34+000339.9	81.7681	0.0611	17.50	16.11	14.74	13.97	1.88	W
SDSS J052705.67+000317.2	81.7736	0.0548	17.53	16.15	14.86	14.09	1.89	W
SDSS J052708.59+001051.7	81.7858	0.1810	20.09	18.68	16.86	15.93	1.77	W
SDSS J052719.49-003928.1	81.8312	-0.6578	16.89	15.49	14.60	14.08	2.59	W
SDSS J052720.93+004623.1	81.8372	0.7731	19.15	17.71	16.22	15.41	1.26	W
SDSS J052725.93+005107.7	81.8581	0.8521	17.32	15.89	14.89	14.26	1.20	C
SDSS J052728.87+003720.9	81.8703	0.6225	18.81	17.37	15.84	15.05	1.40	W
SDSS J052730.70-010716.8	81.8779	-1.1214	19.84	18.33	17.17	16.52	3.05	W
SDSS J052738.25+002303.9	81.9094	0.3844	16.57	15.17	14.25	13.71	1.63	W
SDSS J052749.35+011444.6	81.9557	1.2457	19.15	17.75	16.32	15.51	0.98	W
SDSS J052749.90+000712.4	81.9579	0.1201	17.65	16.26	15.02	14.41	1.89	W
SDSS J052753.54+010831.9	81.9731	1.1422	18.37	17.00	15.51	14.66	1.06	W
SDSS J052754.71+010718.0	81.9780	1.1217	19.24	17.85	16.51	15.77	1.07	W
SDSS J052756.04+001459.5	81.9835	0.2499	19.21	17.87	16.26	15.44	1.79	W
SDSS J052804.23+001237.7	82.0177	0.2105	17.82	16.45	15.16	14.42	1.84	W
SDSS J052805.53+005404.9	82.0231	0.9014	18.21	16.81	15.54	14.80	1.26	W
SDSS J052806.91-001806.0	82.0288	-0.3017	18.47	17.06	15.74	14.98	2.31	W
SDSS J052808.56-011227.3	82.0357	-1.2076	16.72	15.34	14.59	14.21	3.17	W
SDSS J052810.18-004101.5	82.0424	-0.6838	19.47	17.98	16.41	15.45	2.67	W
SDSS J052810.32-000333.0	82.0430	-0.0592	19.18	17.80	16.18	15.26	2.09	W
SDSS J052810.50+000530.7	82.0438	0.0919	18.27	16.88	15.63	14.99	1.95	W
SDSS J052815.12-010259.3	82.0630	-1.0498	18.66	17.24	15.72	14.94	3.03	W
SDSS J052826.91-002505.2	82.1121	-0.4181	18.56	17.12	15.79	15.01	2.45	W
SDSS J052841.84-003556.8	82.1743	-0.5991	17.17	15.79	14.80	14.28	2.64	W
SDSS J052843.04-000008.4	82.1794	-0.0023	18.67	17.35	16.14	15.56	2.10	W
SDSS J052902.29-002606.1	82.2596	-0.4350	19.60	18.12	16.54	15.66	2.52	W
SDSS J052906.11-004127.4	82.2755	-0.6909	17.28	15.88	14.95	14.41	2.76	W
SDSS J052907.90-003105.6	82.2829	-0.5182	18.68	17.07	16.23	15.81	2.61	W
SDSS J052912.90+011340.1	82.3038	1.2278	19.62	18.25	16.76	15.98	1.28	C
SDSS J052930.65-005039.5	82.3777	-0.8443	17.53	16.13	15.27	14.75	2.94	W
SDSS J052939.46-003801.4	82.4144	-0.6337	19.68	18.26	16.57	15.58	2.77	C
SDSS J052952.33-002023.3	82.4681	-0.3398	20.41	18.99	17.15	16.04	2.54	W
SDSS J052957.38+003923.6	82.4891	0.6566	16.71	15.34	14.47	13.97	1.76	W
SDSS J052957.46-003951.8	82.4894	-0.6644	17.69	16.29	15.23	14.62	2.83	W
SDSS J052958.23+004612.6	82.4926	0.7702	18.69	17.23	15.94	15.31	1.69	W
SDSS J052959.50+002728.6	82.4979	0.4580	17.92	16.50	15.31	14.65	1.91	W
SDSS J053010.18-002801.6	82.5424	-0.4671	20.95	19.48	17.63	16.71	2.68	C
SDSS J053010.48+001646.5	82.5437	0.2796	21.14	19.56	17.62	16.59	2.07	C
SDSS J053012.90-003841.4	82.5538	-0.6449	18.89	17.39	15.89	14.99	2.84	W

Table 2—Continued

Name	RA	DEC	<i>g</i>	<i>r</i>	<i>i</i>	<i>z</i>	R <sup>b</sup>	Class <sup>c</sup>
SDSS J053013.39-010049.1	82.5558	-1.0136	19.30	17.91	15.98	14.92	3.17	W
SDSS J053013.77+004519.6	82.5574	0.7554	18.85	17.45	16.57	16.18	1.75	W
SDSS J053019.68-004959.7	82.5820	-0.8333	20.42	18.70	17.02	15.98	3.02	C
SDSS J053026.54+010057.8	82.6106	1.0161	18.15	16.89	15.47	14.65	1.65	C
SDSS J053027.18-011431.1	82.6133	-1.2420	18.33	16.94	15.66	14.96	3.40	W
SDSS J053028.68-002052.2	82.6195	-0.3478	19.47	18.08	16.65	15.86	2.62	C
SDSS J053034.20-001237.8	82.6425	-0.2105	17.86	16.43	15.21	14.53	2.52	W
SDSS J053043.48+005200.5	82.6812	0.8668	19.17	17.75	16.83	16.36	1.79	W
SDSS J053043.60-005236.7	82.6817	-0.8769	20.34	18.97	17.15	16.16	3.11	W
SDSS J053045.44+000905.4	82.6894	0.1515	19.87	18.44	17.01	16.23	2.27	W
SDSS J053047.46-010941.3	82.6978	-1.1615	18.53	17.18	15.79	15.00	3.37	W
SDSS J053056.02+004138.3	82.7334	0.6940	17.89	16.47	15.12	14.40	1.93	W
SDSS J053104.30+005617.7	82.7679	0.9383	19.03	17.51	16.46	16.02	1.82	W
SDSS J053107.98-003318.5	82.7833	-0.5552	19.83	18.23	16.81	15.80	2.89	W
SDSS J053114.19-002230.1	82.8092	-0.3750	21.07	19.47	17.48	16.33	2.75	W
SDSS J053116.57+001239.6	82.8191	0.2110	18.38	16.92	16.05	15.64	2.31	W
SDSS J053121.96+000341.0	82.8415	0.0614	18.26	16.87	15.38	14.58	2.43	W
SDSS J053124.25-010043.9	82.8511	-1.0122	17.24	15.85	14.70	14.01	3.31	W
SDSS J053135.48+004447.2	82.8979	0.7465	18.49	17.00	15.45	14.63	2.03	W
SDSS J053147.19+001205.9	82.9466	0.2016	18.66	17.17	15.69	14.86	2.41	W
SDSS J053147.88-003536.7	82.9495	-0.5935	20.87	19.50	17.68	16.51	3.01	W
SDSS J053206.53+005443.4	83.0272	0.9121	19.43	18.13	16.96	16.38	2.06	W
SDSS J053207.81+001704.9	83.0326	0.2847	19.97	18.08	16.56	15.66	2.42	C
SDSS J053214.90-001102.9	83.0621	-0.1842	19.18	17.76	15.93	14.91	2.76	W
SDSS J053215.50-002637.6	83.0646	-0.4438	19.03	17.65	15.92	15.07	2.96	W
SDSS J053217.88-003141.5	83.0745	-0.5282	18.71	17.00	15.87	15.12	3.03	C
SDSS J053217.95-003107.9	83.0748	-0.5189	16.99	15.60	14.80	14.40	3.03	W
SDSS J053218.47+003148.2	83.0770	0.5301	19.94	18.50	16.79	15.81	2.30	W
SDSS J053219.25-010714.8	83.0802	-1.1208	17.72	16.28	15.10	14.41	3.52	W
SDSS J053219.62-003148.7	83.0818	-0.5302	18.14	16.58	15.45	14.78	3.04	W
SDSS J053221.81-000947.5	83.0909	-0.1632	19.59	18.05	16.59	15.80	2.77	W
SDSS J053223.88-002843.5	83.0995	-0.4788	16.51	15.09	14.26	13.80	3.01	W
SDSS J053224.32-010138.3	83.1014	-1.0273	20.50	18.99	17.32	16.39	3.45	C
SDSS J053225.38-000626.1	83.1058	-0.1073	19.96	18.54	17.20	16.49	2.74	W
SDSS J053228.79-010305.1	83.1200	-1.0514	16.17	14.75	13.74	13.25	3.48	W
SDSS J053229.38-010722.7	83.1224	-1.1230	18.83	17.46	15.67	14.77	3.55	C
SDSS J053232.31-011418.9	83.1347	-1.2386	19.21	17.75	16.17	15.36	3.65	W
SDSS J053234.33-002701.9	83.1431	-0.4505	18.61	17.21	15.56	14.66	3.02	W
SDSS J053237.70-010932.7	83.1571	-1.1591	20.86	19.35	17.69	16.80	3.60	W
SDSS J053238.32-001941.4	83.1597	-0.3282	19.24	17.85	16.18	15.22	2.94	W
SDSS J053238.88-003317.0	83.1620	-0.5547	17.20	15.79	14.74	14.13	3.11	W
SDSS J053239.82-002356.3	83.1659	-0.3990	17.61	16.19	14.94	14.22	2.99	W
SDSS J053241.53-000923.7	83.1731	-0.1566	20.51	19.01	17.17	16.13	2.82	C
SDSS J053249.91-002533.1	83.2080	-0.4259	17.60	15.76	14.88	14.39	3.04	W
SDSS J053250.45-003542.2	83.2102	-0.5951	18.01	16.70	15.32	14.42	3.17	C
SDSS J053300.32-010531.9	83.2514	-1.0922	17.64	16.24	15.06	14.41	3.59	W

Table 2—Continued

Name	RA	DEC	<i>g</i>	<i>r</i>	<i>i</i>	<i>z</i>	R <sup>b</sup>	Class <sup>c</sup>
SDSS J053304.21+000327.0	83.2676	0.0575	19.37	17.91	16.25	15.34	2.74	C
SDSS J053306.33-001555.0	83.2764	-0.2653	17.54	16.12	14.81	14.05	2.97	W
SDSS J053306.56-002254.7	83.2773	-0.3819	16.90	15.55	14.36	13.57	3.06	C
SDSS J053309.15-011028.5	83.2881	-1.1746	18.23	16.80	15.56	14.84	3.68	W
SDSS J053311.20+001358.5	83.2967	0.2329	17.87	16.31	15.04	14.43	2.66	W
SDSS J053311.30-003740.9	83.2971	-0.6280	18.83	17.43	15.92	14.83	3.25	W
SDSS J053317.77-004100.1	83.3241	-0.6834	19.34	17.96	16.47	15.53	3.31	C
SDSS J053323.47+003730.6	83.3478	0.6252	19.18	17.57	16.34	15.74	2.48	W
SDSS J053325.14-005637.0	83.3548	-0.9436	18.51	17.15	15.76	14.97	3.53	W
SDSS J053326.22-004044.3	83.3593	-0.6790	19.39	18.00	16.23	15.22	3.33	W
SDSS J053329.70-011041.9	83.3738	-1.1783	16.73	15.35	14.59	14.18	3.73	W
SDSS J053335.14-005535.1	83.3964	-0.9264	19.63	18.02	16.52	15.60	3.55	C
SDSS J053337.74-005914.3	83.4073	-0.9873	18.30	16.88	15.65	14.90	3.60	W
SDSS J053341.27-002953.7	83.4220	-0.4983	17.05	15.64	14.48	13.84	3.24	W
SDSS J053342.46-000739.0	83.4270	-0.1275	18.43	17.06	15.72	15.01	2.99	W
SDSS J053344.74-004340.4	83.4364	-0.7279	19.62	18.23	16.82	16.02	3.42	W
SDSS J053347.46+003602.4	83.4478	0.6007	19.27	17.84	16.08	15.06	2.58	W
SDSS J053348.95-003921.2	83.4540	-0.6559	18.86	17.38	16.50	15.98	3.38	W
SDSS J053349.04-004625.9	83.4544	-0.7739	16.81	15.44	14.29	13.63	3.47	W
SDSS J053349.05-005520.2	83.4544	-0.9223	16.66	15.28	14.36	13.84	3.58	W
SDSS J053350.20-004239.6	83.4592	-0.7110	19.35	17.94	16.17	15.05	3.42	C
SDSS J053351.78+000028.3	83.4657	0.0079	17.35	15.97	15.01	14.49	2.93	W
SDSS J053400.81+000213.3	83.5034	0.0370	19.12	17.61	16.12	15.16	2.94	C
SDSS J053404.67+010228.5	83.5195	1.0413	18.68	17.37	16.46	16.09	2.47	W
SDSS J053407.28-001626.5	83.5304	-0.2740	19.30	17.88	16.16	15.22	3.16	W
SDSS J053413.50-010720.8	83.5563	-1.1224	17.61	16.19	15.10	14.46	3.80	W
SDSS J053414.22-004243.8	83.5593	-0.7122	20.55	19.04	17.21	16.09	3.49	C
SDSS J053415.29-011519.6	83.5637	-1.2554	17.63	16.19	15.02	14.35	3.91	W
SDSS J053426.37-003351.3	83.6099	-0.5643	18.07	16.68	15.23	14.37	3.42	W
SDSS J053427.01-005422.7	83.6126	-0.9063	19.75	18.29	16.70	15.81	3.67	W
SDSS J053427.15-001242.6	83.6132	-0.2119	17.17	15.71	14.18	13.33	3.18	W
SDSS J053431.08-011112.1	83.6295	-1.1867	18.80	17.38	15.97	15.14	3.90	C
SDSS J053435.44+000340.4	83.6477	0.0612	19.59	18.05	16.50	15.56	3.04	W
SDSS J053441.16+002647.0	83.6715	0.4464	16.63	15.26	14.26	13.69	2.85	W
SDSS J053446.86-002612.6	83.6953	-0.4368	16.48	15.09	14.14	13.57	3.39	W
SDSS J053454.23+000415.4	83.7260	0.0710	17.81	16.38	15.41	14.86	3.10	W
SDSS J053458.20-001502.4	83.7425	-0.2507	19.24	17.83	16.16	15.24	3.31	W
SDSS J053459.45-002717.6	83.7477	-0.4549	20.10	18.71	17.09	16.31	3.44	C
SDSS J053501.77-005954.4	83.7574	-0.9985	17.19	15.80	14.81	14.18	3.83	W
SDSS J053503.57-001511.7	83.7649	-0.2533	19.58	18.16	16.39	15.22	3.32	W
SDSS J053506.59-002108.3	83.7775	-0.3523	20.04	18.54	16.72	15.67	3.40	W
SDSS J053515.61-003442.2	83.8151	-0.5784	20.89	19.31	17.47	16.31	3.58	W
SDSS J053518.00-001742.1	83.8250	-0.2950	19.56	18.19	16.39	15.41	3.40	W
SDSS J053525.22-004324.3	83.8551	-0.7234	18.21	16.52	15.26	14.43	3.70	W
SDSS J053527.88+001025.0	83.8662	0.1736	18.81	17.40	16.11	15.42	3.16	W
SDSS J053532.90+000214.2	83.8871	0.0373	20.41	19.00	17.40	16.54	3.25	W

Table 2—Continued

Name	RA	DEC	<i>g</i>	<i>r</i>	<i>i</i>	<i>z</i>	R <sup>b</sup>	Class <sup>c</sup>
SDSS J053532.98-003114.1	83.8874	-0.5206	17.78	16.37	15.13	14.46	3.59	W
SDSS J053536.66-000459.4	83.9028	-0.0832	20.59	19.16	17.38	16.32	3.33	W
SDSS J053537.51-010624.0	83.9063	-1.1067	19.06	17.62	16.23	15.47	4.02	W
SDSS J053538.51-005111.5	83.9105	-0.8532	19.38	17.67	16.06	15.27	3.84	C
SDSS J053543.97-005609.7	83.9332	-0.9361	17.53	16.13	14.89	14.13	3.91	W
SDSS J053544.61-001426.4	83.9359	-0.2407	16.78	15.39	14.46	13.94	3.45	W
SDSS J053551.70-000956.0	83.9654	-0.1656	18.90	17.38	15.76	14.81	3.43	W
SDSS J053555.54+003339.0	83.9814	0.5608	20.56	19.06	17.36	16.41	3.07	C
SDSS J053557.13-003933.6	83.9881	-0.6594	19.30	17.93	16.44	15.61	3.76	W
SDSS J053600.82+010716.7	84.0034	1.1213	18.85	17.34	16.43	15.96	2.91	W
SDSS J053609.19-002632.1	84.0383	-0.4422	18.14	16.74	15.29	14.48	3.66	W
SDSS J053610.40-004039.1	84.0433	-0.6775	19.53	18.12	16.63	15.83	3.81	W
SDSS J053618.37+003644.6	84.0766	0.6124	19.17	17.83	16.42	15.64	3.14	W
SDSS J053623.67+000041.6	84.0986	0.0116	20.11	18.71	17.28	16.58	3.44	W
SDSS J053642.89-004508.3	84.1787	-0.7523	18.79	17.40	15.81	14.91	3.96	W
SDSS J053650.26+003654.8	84.2094	0.6152	19.56	18.09	16.84	16.18	3.26	W
SDSS J053650.72+000742.3	84.2114	0.1284	17.85	16.45	15.21	14.54	3.48	W
SDSS J053655.09-003022.9	84.2296	-0.5064	17.89	16.50	15.24	14.55	3.85	W
SDSS J053701.00-005512.3	84.2542	-0.9201	19.02	17.68	16.23	15.44	4.13	W
SDSS J053704.36+005516.2	84.2682	0.9212	18.27	17.30	15.55	14.66	3.22	W
SDSS J053704.83-005814.1	84.2702	-0.9706	19.12	17.65	16.26	15.46	4.18	W
SDSS J053704.97-000812.4	84.2707	-0.1368	19.89	18.45	16.74	15.87	3.67	W
SDSS J053709.92-011050.4	84.2913	-1.1807	18.74	17.37	15.77	14.92	4.34	W
SDSS J053710.85+010423.1	84.2952	1.0731	19.70	18.25	16.79	15.96	3.20	W
SDSS J053716.27-010336.5	84.3178	-1.0602	21.26	19.84	17.76	16.70	4.27	C
SDSS J053719.30+010555.0	84.3304	1.0986	19.21	17.77	16.20	15.24	3.23	W
SDSS J053723.38-010344.3	84.3474	-1.0623	16.57	15.18	14.22	13.67	4.30	W
SDSS J053724.24-002350.4	84.3510	-0.3973	19.19	17.79	16.48	15.75	3.88	W
SDSS J053725.62-003206.4	84.3568	-0.5351	19.54	17.96	16.64	15.77	3.96	C
SDSS J053729.79+000540.9	84.3741	0.0947	17.65	16.13	15.22	14.75	3.64	W
SDSS J053729.80-002414.4	84.3742	-0.4040	17.26	15.86	14.53	13.78	3.90	W
SDSS J053729.83+010124.6	84.3743	1.0235	21.16	19.84	17.94	16.74	3.29	C
SDSS J053730.46+004104.0	84.3769	0.6845	17.75	16.34	15.11	14.39	3.39	W
SDSS J053731.91-001916.8	84.3830	-0.3214	19.38	17.47	16.02	15.22	3.86	C
SDSS J053735.75-002640.3	84.3990	-0.4445	20.43	19.04	17.33	16.48	3.94	W
SDSS J053737.35-002827.8	84.4057	-0.4744	19.61	18.17	16.28	15.26	3.97	W
SDSS J053738.97-004656.4	84.4124	-0.7823	19.48	18.03	16.37	15.46	4.16	W
SDSS J053742.93+002434.5	84.4289	0.4096	17.46	16.05	15.12	14.55	3.54	W
SDSS J053747.50+011540.9	84.4479	1.2614	17.07	15.72	14.88	14.39	3.31	W
SDSS J053747.92-000603.9	84.4497	-0.1011	19.50	18.09	16.53	15.71	3.80	W
SDSS J053749.15+000923.6	84.4548	0.1566	19.59	18.18	16.62	15.77	3.68	W
SDSS J053750.64+004322.3	84.4610	0.7229	19.68	18.30	16.80	16.00	3.46	W
SDSS J053752.16+005827.1	84.4674	0.9742	19.26	16.78	15.53	14.85	3.39	W
SDSS J053758.23+003155.3	84.4926	0.5320	17.33	15.94	14.76	14.07	3.56	W
SDSS J053801.02-010858.3	84.5043	-1.1496	19.63	18.06	16.47	15.57	4.47	W
SDSS J053801.50+000701.5	84.5063	0.1171	18.17	16.77	15.50	14.78	3.74	W

Table 2—Continued

Name	RA	DEC	<i>g</i>	<i>r</i>	<i>i</i>	<i>z</i>	R <sup>b</sup>	Class <sup>c</sup>
SDSS J053806.65+002251.1	84.5277	0.3809	17.79	16.39	15.19	14.52	3.65	W
SDSS J053806.74-010817.8	84.5281	-1.1383	20.41	19.01	17.23	16.10	4.48	W
SDSS J053808.51-001156.3	84.5355	-0.1990	19.94	18.57	16.74	15.77	3.92	W
SDSS J053812.51-000908.8	84.5522	-0.1525	17.04	15.61	14.66	14.08	3.91	W
SDSS J053812.72-001228.1	84.5530	-0.2078	17.55	16.14	14.93	14.23	3.94	C
SDSS J053817.30-010010.5	84.5721	-1.0029	18.90	17.49	15.72	14.68	4.42	C
SDSS J053821.31-001830.4	84.5888	-0.3085	20.10	18.67	16.89	15.88	4.03	W
SDSS J053829.54-004104.8	84.6231	-0.6847	17.95	16.56	15.11	14.21	4.27	W
SDSS J053835.53-001221.5	84.6481	-0.2060	20.47	18.95	17.21	16.06	4.02	C
SDSS J053837.34+001948.9	84.6556	0.3303	19.34	17.84	16.65	15.93	3.78	C
SDSS J053839.62+001407.9	84.6651	0.2356	20.59	19.14	17.31	16.34	3.83	W
SDSS J053841.68-000234.4	84.6737	-0.0429	18.17	16.82	15.61	14.90	3.96	W
SDSS J053846.10-004620.5	84.6921	-0.7724	19.75	18.34	16.37	15.20	4.38	W
SDSS J053848.20-000051.0	84.7009	-0.0142	17.74	16.38	15.19	14.46	3.98	W
SDSS J053851.37-002429.4	84.7141	-0.4082	19.87	18.43	16.94	16.09	4.19	W
SDSS J053853.84-004920.0	84.7244	-0.8222	17.51	16.14	14.64	13.56	4.43	W
SDSS J053904.29-003810.0	84.7679	-0.6361	18.19	16.76	15.34	14.48	4.36	W
SDSS J053908.87+003045.3	84.7870	0.5126	18.85	17.48	15.79	14.91	3.84	W
SDSS J053909.18-002353.3	84.7883	-0.3982	17.52	16.17	15.06	14.37	4.24	W
SDSS J053914.59-011124.4	84.8108	-1.1901	17.53	16.15	15.24	14.75	4.73	W
SDSS J053914.96+010959.5	84.8124	1.1665	18.13	16.66	15.48	14.75	3.69	W
SDSS J053918.17+011132.8	84.8257	1.1925	18.90	17.39	16.51	16.02	3.69	W
SDSS J053918.74-001305.3	84.8281	-0.2182	18.77	17.35	16.04	15.23	4.18	W
SDSS J053919.91+010138.6	84.8330	1.0274	18.82	16.97	16.14	15.70	3.73	C
SDSS J053925.88+011334.6	84.8578	1.2263	19.09	17.64	16.56	15.92	3.72	W
SDSS J053938.75+010947.1	84.9115	1.1631	19.77	18.32	16.72	15.84	3.78	W
SDSS J053940.26-003149.9	84.9178	-0.5305	19.42	17.68	16.58	15.91	4.42	C
SDSS J053941.02-001716.8	84.9210	-0.2880	18.59	17.15	15.82	15.08	4.30	C
SDSS J053941.76-011435.6	84.9240	-1.2432	19.31	17.84	16.28	15.39	4.85	W
SDSS J053950.20+001748.2	84.9592	0.2967	19.19	17.78	16.34	15.53	4.08	W
SDSS J053952.65+001406.4	84.9694	0.2351	20.30	18.55	17.08	16.33	4.11	W
SDSS J054010.45+001729.7	85.0436	0.2916	19.77	18.33	16.84	16.10	4.16	W
SDSS J054021.92-001906.9	85.0913	-0.3186	18.44	17.03	15.76	15.06	4.46	W
SDSS J054048.80+010056.2	85.2034	1.0156	18.42	17.41	15.93	15.30	4.10	W
SDSS J054058.03+003329.0	85.2418	0.5581	17.05	15.66	14.79	14.28	4.25	W
SDSS J054059.22+011107.4	85.2468	1.1854	20.70	19.23	17.52	16.59	4.11	W
SDSS J054103.34-004213.5	85.2639	-0.7038	16.91	15.52	14.24	13.47	4.81	W
SDSS J054105.34+011336.8	85.2723	1.2269	18.13	16.80	15.48	14.81	4.13	W
SDSS J054107.73+001453.6	85.2822	0.2482	19.18	17.79	16.24	15.54	4.39	C
SDSS J054113.59+003930.1	85.3066	0.6584	19.34	17.67	16.75	16.30	4.29	W
SDSS J054118.28-002213.9	85.3262	-0.3705	19.48	18.02	16.64	15.88	4.69	W
SDSS J054119.72+001849.2	85.3322	0.3137	18.73	17.31	16.12	15.45	4.42	W
SDSS J054123.09-000854.3	85.3462	-0.1484	18.51	17.10	15.77	15.05	4.61	W
SDSS J054123.86-010408.7	85.3495	-1.0691	18.76	17.42	15.81	14.99	5.08	W
SDSS J054128.86+003951.7	85.3703	0.6644	17.73	16.05	15.09	14.51	4.35	W
SDSS J054144.34-003519.1	85.4348	-0.5887	18.95	17.43	15.97	15.05	4.90	W

Table 2—Continued

Name	RA	DEC	<i>g</i>	<i>r</i>	<i>i</i>	<i>z</i>	R <sup>b</sup>	Class <sup>c</sup>
SDSS J054145.35+001256.3	85.4390	0.2157	16.91	15.62	14.96	14.65	4.55	W
SDSS J054200.37-004528.5	85.5016	-0.7579	21.10	19.69	17.53	16.17	5.04	W
SDSS J054204.19+010908.9	85.5175	1.1525	20.00	18.40	17.31	16.70	4.38	W
SDSS J054220.47-010424.9	85.5853	-1.0736	18.17	16.66	15.69	15.21	5.28	W
SDSS J054227.25-010924.4	85.6136	-1.1568	19.12	17.64	16.26	15.50	5.35	W
SDSS J054227.45-010315.9	85.6144	-1.0544	17.51	15.73	14.81	14.30	5.29	W
SDSS J054228.10-010349.3	85.6171	-1.0637	18.26	16.80	16.02	15.60	5.30	W
SDSS J054228.64-000044.4	85.6193	-0.0123	19.16	17.61	16.60	15.99	4.80	W
SDSS J054229.09-010321.5	85.6212	-1.0560	15.88	14.59	13.89	13.56	5.30	W
SDSS J054230.98-000126.9	85.6291	-0.0241	20.24	18.59	16.56	15.44	4.82	W
SDSS J054233.34-002550.4	85.6389	-0.4307	18.06	16.70	15.31	14.50	5.00	W
SDSS J054238.76-011025.6	85.6615	-1.1738	19.26	17.25	16.19	15.50	5.40	W
SDSS J054244.57-010446.8	85.6857	-1.0797	17.69	15.40	14.25	13.46	5.37	W
SDSS J054251.34+010206.8	85.7139	1.0352	18.97	17.49	16.14	15.21	4.60	C
SDSS J054254.19-010506.3	85.7258	-1.0851	20.58	18.17	16.64	15.56	5.40	W
SDSS J054303.64+000631.3	85.7652	0.1087	17.13	15.74	15.13	14.88	4.90	W
SDSS J054305.68+001453.6	85.7737	0.2482	16.75	15.36	14.38	13.83	4.86	C
SDSS J054306.32+005223.8	85.7764	0.8733	18.26	16.76	15.32	14.46	4.69	W
SDSS J054309.71+001202.2	85.7905	0.2006	20.62	19.12	17.37	16.43	4.89	W
SDSS J054311.76-003539.8	85.7990	-0.5944	20.47	18.91	17.43	16.48	5.22	W
SDSS J054319.67+000528.6	85.8320	0.0913	18.89	17.33	16.53	16.09	4.96	W
SDSS J054333.48-010057.9	85.8895	-1.0161	19.12	17.24	16.12	15.46	5.50	C
SDSS J054344.49+010406.4	85.9354	1.0684	20.10	18.52	17.32	16.71	4.81	W
SDSS J054348.41+001937.5	85.9518	0.3271	18.58	17.18	16.03	15.36	5.00	W
SDSS J054350.07+004454.4	85.9586	0.7484	18.12	16.65	15.54	14.97	4.89	W
SDSS J054351.87+003639.0	85.9661	0.6109	17.18	15.79	14.48	13.67	4.93	W
SDSS J054358.43-004438.0	85.9935	-0.7439	19.51	17.49	16.22	15.36	5.46	W
SDSS J054424.87+010815.2	86.1037	1.1376	18.93	17.37	16.56	16.09	4.97	W
SDSS J054428.06-010525.3	86.1169	-1.0904	20.03	17.72	16.29	15.34	5.74	W
SDSS J054435.59-010107.2	86.1483	-1.0187	20.12	18.09	16.85	16.02	5.73	W
SDSS J054437.55-001650.9	86.1565	-0.2808	17.67	16.26	15.26	14.69	5.40	W
SDSS J054450.07-003017.9	86.2086	-0.5050	20.65	19.12	17.20	16.15	5.54	C
SDSS J054454.86-004055.1	86.2286	-0.6820	19.53	17.57	16.60	15.97	5.64	W
SDSS J054501.89+000630.9	86.2579	0.1086	19.93	18.33	16.49	15.39	5.36	W
SDSS J054503.46+003454.6	86.2644	0.5818	20.45	18.93	17.11	16.12	5.23	W
SDSS J054504.38+003712.0	86.2683	0.6200	19.58	18.14	16.38	15.45	5.23	W
SDSS J054509.50+005418.3	86.2896	0.9051	20.51	19.02	17.11	16.03	5.19	W
SDSS J054510.17-003512.3	86.2924	-0.5868	19.22	17.66	16.09	14.98	5.65	C
SDSS J054526.16+000637.9	86.3590	0.1105	17.78	16.30	14.85	14.06	5.45	W
SDSS J054538.90-004555.8	86.4121	-0.7655	20.32	18.85	17.24	16.34	5.84	W
SDSS J054544.64+001300.5	86.4360	0.2168	16.49	15.09	14.30	13.87	5.49	W
SDSS J054557.93+000248.5	86.4914	0.0468	19.66	18.20	16.53	15.49	5.60	C
SDSS J054559.34+002920.7	86.4973	0.4891	16.50	14.99	13.70	13.06	5.48	W
SDSS J054600.17+000307.1	86.5007	0.0520	18.34	16.67	14.88	13.87	5.61	W
SDSS J054601.37-000013.6	86.5057	-0.0038	19.29	17.27	16.02	15.24	5.63	C
SDSS J054604.92+000145.5	86.5205	0.0293	18.70	16.79	15.58	14.76	5.63	W

Table 2—Continued

Name	RA	DEC	<i>g</i>	<i>r</i>	<i>i</i>	<i>z</i>	R <sup>b</sup>	Class <sup>c</sup>
SDSS J054606.02+003702.6	86.5251	0.6174	17.95	16.41	15.29	14.73	5.48	W
SDSS J054608.66+000454.3	86.5361	0.0818	20.30	17.92	16.50	15.49	5.63	W
SDSS J054609.26+001332.5	86.5386	0.2257	16.94	15.29	14.16	13.57	5.59	C
SDSS J054621.44+000454.7	86.5894	0.0819	17.15	15.64	14.87	14.62	5.68	W
SDSS J054625.88+000931.8	86.6079	0.1589	19.54	17.82	16.25	15.21	5.68	C
SDSS J054626.65+003107.3	86.6111	0.5187	19.85	17.46	16.03	14.95	5.58	C
SDSS J054638.40+001511.5	86.6600	0.2532	21.64	19.47	17.09	15.69	5.70	C
SDSS J054638.57+002205.9	86.6607	0.3683	21.13	18.63	16.91	15.73	5.67	C
SDSS J054639.14-000914.9	86.6631	-0.1541	18.02	15.58	14.07	13.15	5.83	W
SDSS J054640.77+002722.7	86.6699	0.4563	20.35	18.48	16.58	15.17	5.65	C
SDSS J054645.31-002943.6	86.6888	-0.4955	18.59	16.50	15.30	14.51	5.98	W
SDSS J054650.16-000342.1	86.7090	-0.0617	18.10	15.73	14.30	13.26	5.84	W
SDSS J054651.33+003225.6	86.7139	0.5405	18.51	16.09	14.65	13.64	5.68	W
SDSS J054652.92+005929.3	86.7205	0.9915	19.48	18.03	16.86	16.17	5.60	W
SDSS J054656.54+002052.7	86.7356	0.3480	18.24	16.11	14.84	13.95	5.75	W
SDSS J054706.48-005916.0	86.7770	-0.9878	19.66	17.32	15.97	15.12	6.27	W
SDSS J054706.98+003155.9	86.7791	0.5322	20.76	18.43	16.65	15.44	5.74	C
SDSS J054716.95+003719.0	86.8206	0.6220	20.62	18.00	16.40	15.23	5.76	W
SDSS J054717.16+001824.5	86.8215	0.3068	19.87	17.91	16.40	15.37	5.84	C
SDSS J054719.18+001920.5	86.8299	0.3224	20.58	18.20	16.50	15.48	5.84	C
SDSS J054721.17-005736.7	86.8382	-0.9602	19.55	16.80	15.21	14.16	6.31	W
SDSS J054724.89-005350.9	86.8537	-0.8975	19.88	18.32	17.05	16.39	6.29	W
SDSS J054728.28-010002.0	86.8679	-1.0006	20.20	17.80	16.54	15.70	6.35	W
SDSS J054733.78-003106.1	86.8908	-0.5184	18.19	16.59	15.33	14.64	6.17	W
SDSS J054743.22-010032.4	86.9301	-1.0090	20.45	18.00	16.67	15.86	6.41	W
SDSS J054744.99+003841.8	86.9375	0.6450	19.69	16.77	14.92	13.63	5.87	W
SDSS J054747.30+002226.3	86.9471	0.3740	19.65	17.14	15.82	14.91	5.94	W
SDSS J054748.05-010148.0	86.9502	-1.0300	19.87	17.41	16.09	15.32	6.44	W
SDSS J054748.63+004707.7	86.9527	0.7855	20.84	18.25	16.80	15.75	5.86	W
SDSS J054750.11+004154.5	86.9588	0.6985	19.59	17.88	16.55	15.89	5.88	W
SDSS J054750.34+004702.7	86.9598	0.7841	18.42	16.69	15.81	15.32	5.87	W
SDSS J054753.30+010219.1	86.9721	1.0387	19.90	17.96	16.77	15.96	5.84	W
SDSS J054753.66+004320.4	86.9736	0.7224	18.22	16.58	15.18	14.45	5.89	W
SDSS J054754.35-005317.7	86.9765	-0.8883	19.80	16.48	14.72	13.39	6.40	W
SDSS J054754.42-003907.6	86.9768	-0.6521	18.76	17.29	16.07	15.38	6.30	W
SDSS J054754.83+001538.6	86.9785	0.2607	18.23	16.69	15.73	15.26	6.00	W
SDSS J054755.78-005902.0	86.9824	-0.9839	20.83	18.36	17.13	16.26	6.45	W
SDSS J054758.01+001341.0	86.9917	0.2281	19.81	17.98	17.00	16.38	6.02	W
SDSS J054802.14+004940.9	87.0089	0.8280	19.29	16.84	15.61	14.73	5.91	W
SDSS J054807.22+004908.1	87.0301	0.8189	19.24	17.22	16.17	15.51	5.93	W
SDSS J054808.67+002153.9	87.0362	0.3650	19.61	17.51	16.53	15.91	6.03	W
SDSS J054809.64+002246.5	87.0402	0.3796	20.36	18.08	16.96	16.23	6.03	W
SDSS J054811.78+004152.9	87.0491	0.6980	19.86	17.80	16.65	15.89	5.97	W
SDSS J054814.57-005645.5	87.0607	-0.9460	20.02	18.52	16.72	15.69	6.50	W
SDSS J054817.78-003917.7	87.0741	-0.6549	17.71	16.29	14.85	13.96	6.40	W
SDSS J054842.62-002313.5	87.1776	-0.3871	20.10	18.64	17.04	16.14	6.39	W

Table 2—Continued

Name	RA	DEC	<i>g</i>	<i>r</i>	<i>i</i>	<i>z</i>	R <sup>b</sup>	Class <sup>c</sup>
SDSS J054851.07-003006.0	87.2128	-0.5017	17.53	16.13	15.43	15.12	6.47	W
SDSS J054909.75-010829.3	87.2907	-1.1415	20.44	17.62	16.01	14.81	6.79	W
SDSS J054914.57-000714.8	87.3107	-0.1208	17.69	16.29	15.35	14.90	6.43	W
SDSS J054943.60+005638.6	87.4317	0.9441	18.69	17.12	16.04	15.44	6.31	C
SDSS J054946.93+003102.8	87.4456	0.5175	18.09	15.74	14.31	13.40	6.40	W
SDSS J054952.28-001147.9	87.4679	-0.1966	18.81	17.35	16.14	15.51	6.60	W
SDSS J054956.21-0004843.7	87.4842	-0.8122	19.12	17.71	15.96	15.00	6.83	W
SDSS J054958.08+000417.7	87.4920	0.0716	21.26	19.36	17.48	16.33	6.55	C
SDSS J054959.02+005550.5	87.4959	0.9307	19.74	18.22	16.76	15.95	6.37	W
SDSS J055004.32+005624.3	87.5180	0.9401	18.75	17.14	16.24	15.88	6.39	W
SDSS J055005.55+002305.7	87.5232	0.3849	19.14	17.63	15.93	14.97	6.50	W
SDSS J055010.21+010156.0	87.5426	1.0322	18.32	16.96	15.92	15.63	6.40	W
SDSS J055010.38-000241.3	87.5433	-0.0448	19.36	17.53	16.11	15.26	6.63	W
SDSS J055020.01+001032.6	87.5834	0.1757	20.72	19.06	17.03	15.84	6.61	W
SDSS J055038.14+002232.0	87.6590	0.3756	20.45	18.96	17.34	16.44	6.63	W
SDSS J055041.06-011201.0	87.6711	-1.2003	18.69	17.33	16.21	15.71	7.16	W
SDSS J055115.65+003911.4	87.8152	0.6532	18.07	16.58	15.23	14.49	6.73	W
SDSS J055124.33-010512.6	87.8514	-1.0869	18.12	16.65	15.62	15.10	7.28	W
SDSS J055124.86-005109.2	87.8536	-0.8526	18.53	16.81	15.88	15.32	7.19	W
SDSS J055133.61-010651.4	87.8901	-1.1143	18.09	16.60	15.54	14.99	7.33	W
SDSS J055135.15+000120.5	87.8965	0.0224	19.33	17.82	16.60	15.97	6.95	W
SDSS J055135.72-010322.2	87.8989	-1.0562	15.86	14.18	13.41	13.01	7.31	W
SDSS J055211.45+011119.8	88.0477	1.1889	19.07	17.37	16.35	15.68	6.89	W
SDSS J055237.20+002431.9	88.1550	0.4089	17.81	16.34	15.20	14.54	7.11	W
SDSS J055238.73-002614.8	88.1614	-0.4375	18.29	16.80	15.62	15.00	7.34	W
SDSS J055244.28-002526.5	88.1845	-0.4240	19.29	17.69	16.67	16.11	7.35	W
SDSS J055255.95+002125.6	88.2331	0.3571	18.69	17.26	15.91	15.16	7.20	W
SDSS J055341.87-004041.1	88.4245	-0.6781	20.66	18.78	17.55	16.79	7.66	W
SDSS J055401.49-004411.9	88.5062	-0.7367	18.38	16.93	15.75	15.13	7.76	W
SDSS J055452.48+011138.3	88.7187	1.1940	19.45	17.98	16.63	15.96	7.56	C
SDSS J055505.24-004508.8	88.7718	-0.7524	19.41	17.95	16.67	15.98	8.02	W
SDSS J055512.26+002408.3	88.8011	0.4023	19.47	18.09	16.74	16.01	7.75	W
SDSS J055552.60-001945.9	88.9692	-0.3294	17.64	16.22	15.01	14.34	8.08	W
SDSS J055623.10-004419.7	89.0963	-0.7388	19.88	17.91	16.80	16.12	8.32	W
SDSS J055629.02+004835.3	89.1209	0.8098	19.54	18.09	16.48	15.62	8.00	W
SDSS J055631.89-002110.1	89.1329	-0.3528	20.23	18.63	17.26	16.51	8.24	W
SDSS J055734.48-001356.4	89.3937	-0.2324	20.39	18.86	17.38	16.54	8.46	W
SDSS J055742.29-005017.2	89.4262	-0.8381	19.98	18.57	17.26	16.59	8.66	W
SDSS J055742.93-010234.1	89.4289	-1.0428	19.13	17.58	16.65	16.17	8.73	W
SDSS J055801.82-000303.8	89.5076	-0.0511	20.53	19.06	17.26	16.20	8.53	W
SDSS J055806.59-004946.0	89.5275	-0.8295	19.09	17.65	16.10	15.29	8.76	W
SDSS J055823.09+000405.9	89.5962	0.0683	17.23	15.77	14.31	13.50	8.59	W
SDSS J055835.30-004729.1	89.6471	-0.7914	20.73	19.13	17.75	16.97	8.86	C
SDSS J055854.84+005636.6	89.7285	0.9435	19.20	17.75	16.26	15.47	8.59	W
SDSS J055912.55-002947.3	89.8023	-0.4965	19.42	17.68	16.72	16.13	8.93	W
SDSS J055938.44+004035.7	89.9102	0.6766	17.25	15.81	15.04	14.73	8.80	W

Table 2—Continued

Name	RA	DEC	<i>g</i>	<i>r</i>	<i>i</i>	<i>z</i>	R <sup>b</sup>	Class <sup>c</sup>
------	----	-----	----------	----------	----------	----------	----------------	--------------------

<sup>a</sup>Distance in degrees from the Be star 25 Orionis.

<sup>b</sup>Preliminary classification as WTTS (W) or CTTS (C) based on multi-band variability.